



Cite this: *Sustainable Energy Fuels*, 2023, 7, 2178

## Greenhouse gas emission reduction and energy impact of electrifying upgraders in refineries using plasma processing technology

Shariful Islam Bhuiyan, <sup>a</sup> Jamie Kraus, <sup>a</sup> Md Abdullah Hil Baky, <sup>a</sup> Rollie Stanich, <sup>b</sup> Kunpeng Wang, <sup>b</sup> Howard Jemison <sup>b</sup> and David Staack <sup>\*a</sup>

Climate change and global warming are happening at an alarming rate. Meanwhile, conventional oil reserves are also being depleted. With the increasing energy demand, a new climate-positive pathway is essential to transition from CO<sub>2</sub>-intensive thermal processes in refineries to greener processes with reduced emissions. Electrifying upgraders in refineries using a plasma processing technology integrated with renewable energy provides an attractive solution to process hydrocarbons with minimal emissions. This paper evaluates the energy requirements, associated greenhouse gas emissions, and energy economics of using plasma processing technology for heavy oil upgrading in refineries by replacing the fluid catalytic cracker unit using a model called petroleum refinery life cycle inventory model. The plasma calculations were performed based on bench-scale laboratory experimental results assuming similar conversion and linear scaleup. Two refinery configurations were analyzed and compared with the plasma processing technology. The first refinery configuration comprised of a traditional medium refinery with West Texas Intermediate as the crude oil input while the second comprised of a traditional deep refinery with LloyDMINSTER Blend as the crude oil input. Implementing plasma processing technology increases energy consumption by 18% in the medium refinery and 14% in the deep refinery which translates to <2% energy content of a barrel of oil. The greenhouse gas emissions were reduced significantly with 21% reduction for medium and 35% reduction for deep refinery configuration. With a carbon tax incorporated, plasma processing technology increases the energy consumption cost by <\$0.30 per barrel. A sensitivity analysis performed shows that varying the renewable energy cost, carbon tax, specific energy input to plasma for similar conversion, and plasma processing hydrogen yield can make plasma processing technology an economically feasible and competitive model. Finally, the life cycle assessment and the well to tank analysis were conducted for the plasma deep refinery configuration. Electrifying upgraders using plasma in a deep refinery reduces emissions from 166 kg CO<sub>2eq</sub> per barrel of bitumen for the entire life cycle from the well to tank to 148 kg CO<sub>2eq</sub> per barrel, a reduction of 11.5%. Integrating such technology in just 3% of United States refineries can reduce emissions by 2 million metric ton CO<sub>2eq</sub> per year, a significant milestone toward energy transition.

Received 5th August 2022  
Accepted 17th January 2023

DOI: 10.1039/d2se01089e  
[rsc.li/sustainable-energy](http://rsc.li/sustainable-energy)

## 1. Introduction

In 2019, the world consumed about 100 million barrels of petroleum per day, while the United States (US) consumed an average of 20.54 million barrels of petroleum.<sup>1</sup> The greenhouse gas reporting program reported that the refinery sector in the US emits ~175 million metric ton of CO<sub>2eq</sub> per year.<sup>1</sup> Meanwhile, conventional energy resources are declining, and hence unconventional resources are becoming important in addressing the increasing energy demand. However, unconventional oil resources face tough challenges, as they have higher energy

consumption per unit of fuel produced compared to conventional petroleum.<sup>2,3</sup> Climate change, ecological issues, water consumption, and air pollution are some of the concerns that do not favor the expansion of unconventional resources. The production (extraction, transport, refining, *etc.*) of unconventional oil resources often have a higher energy intensity requirement than conventional oil resources, therefore resulting in higher greenhouse gas (GHG) emissions. Climate policies such as the low carbon fuel standard,<sup>4</sup> the European fuel quality directive,<sup>5</sup> and the Alberta specified gas emitter regulation<sup>6</sup> are adding strict regulations for reducing GHG emissions. Hence, alternate pathways are required such that refining heavy oil results in reduced emissions. One such energy transition pathway is electrifying process units in refineries, such as the fluid catalytic cracker (FCC) unit. Plasma processing technology

<sup>a</sup>Mechanical Engineering, Texas A&M University, College Station, TX, 77843, USA.  
E-mail: [dstaack@tamu.edu](mailto:dstaack@tamu.edu)

<sup>b</sup>LTEOIL, LLC, 2929 Allen Parkway, Suite 200, Houston, TX, 77019, USA



(PPT) is a novel technology that can be powered by renewable energy to upgrade heavy oils and produce hydrogen simultaneously. Considerable work has been performed to investigate different plasma upgrading technologies for higher conversions at a laboratory scale, with promising results. However, no work has been performed to map out these technologies at an industrial scale, and evaluate their energy consumption, environmental footprint, and cost analysis.

This paper evaluates the energy consumption, GHG emissions, and energy cost of one such novel PPT by implementing it at an industrial scale in different refinery configurations by replacing the FCC to convert and upgrade heavy oils. This is performed in two refinery configurations. The first refinery configuration consists of a traditional medium refinery (TMR) where the FCC is replaced by the PPT, and the input crude oil is West Texas Intermediate (WTI). This refinery configuration is called plasma medium refinery (PMR). The second refinery consists of a traditional deep refinery (TDR) where the FCC is also replaced by the PPT, but the input crude oil is Lloydminster Blend (LLB). This refinery configuration is called plasma deep refinery (PDR). A linear scaleup calculation is performed to compare and match the FCC and PPT for similar conversion based on published experimental results.<sup>7</sup> A sensitivity analysis is also performed on the energy cost of the two technologies by varying the renewable energy cost, carbon tax, specific energy input to plasma for similar conversion, and plasma processing hydrogen yield. Finally, a life cycle assessment (LCA) and well-to-tank (WTT) analysis is also performed for the PDR configuration.

### 1.1. Previous LCA studies for greenhouse gas emissions

Several studies have been conducted to examine the LCA and GHG emissions of heavy oil upgrading and other carbon emitting processes.<sup>8–12</sup> Nimana *et al.* estimated the specific energy consumption and GHG emissions for upgrading bitumen to synthetic crude oil (SCO)<sup>13</sup> and concluded that hydroconversion is more energy and GHG intensive than delayed coker upgrading. Nduagu *et al.* compared the energy intensities and GHG emissions of unconventional oils alongside shale gas, coal, lignite, wood, and conventional oil and gas.<sup>14</sup> It was estimated that 4–21 metric gigaton-CO<sub>2eq</sub> of GHG would be emitted over the next four decades (2010–2050) if the growth of unconventional heavy oil production continued at the same rate. Charry Sanchez *et al.* presented a new energy optimization model for oil sand upgrading operations.<sup>15</sup> The mathematical model selected the bitumen upgrader plants most suitable for minimizing the annual energy costs while meeting CO<sub>2</sub> emission constraints and found the most suitable upgrading plant to be hydrocracking based. Nimana *et al.* also performed a comprehensive LCA for transportation fuels and analyzed all the current possible pathways from bitumen extraction to use in vehicles.<sup>16</sup> Life cycle well-to-wheel (WTW) emissions ranged from 106.8 to 116 g CO<sub>2eq</sub> per MJ of gasoline, 100.5 to 115.2 g CO<sub>2eq</sub> per MJ of diesel, and 96.4 to 109.2 g-CO<sub>2eq</sub> per MJ of jet fuel, depending on the pathway.

Similarly, LCA studies on other plasma applications have also been researched. Delikostantis *et al.* analyzed the

sustainability of plasma-assisted ethylene production from methane rich gas streams, mainly natural gas and shale gas.<sup>17</sup> They concluded that the two-step process of conversion to acetylene followed by acetylene to ethylene hydrogenation, powered by electricity *via* wind turbines, had the lowest carbon footprint scenario. They also modeled the process of plasma-assisted ethylene production from methane and concluded that plasma-assisted processes can become viable if electricity costs go down.<sup>18</sup> Another LCA of the nitrogen fixation process, assisted by plasma technology and incorporating renewable energy, was performed by Anastasopoulou *et al.*<sup>19</sup> The results showed that optimization leads to an improvement of 19% in global warming potential compared to a conventional production pathway when equipped with plasma-assisted nitric acid and renewable energy.

### 1.2. Overview of heavy oil processing

Currently, Canadian crude and oil sands are commercialized as diluted bitumen or synthetic crude oil (SCO).<sup>20,21</sup> After extraction, bitumen is blended with diluents and shipped to US refineries designed to process heavy oil. Upgrading is a process by which crude oil is treated to yield a higher value product, generally with the help of heat and catalysts, using thermal cracking processes. Large-scale commercial upgrading technologies comprise either catalytic thermal cracking, coking technologies, or catalytic hydroconversion technologies. Thermal cracking is based on the use of thermal energy to break bonds and convert them into lighter components. Hydrocracking also uses thermal energy with a catalyst present to break the large hydrocarbon chains into smaller compounds, such as naphtha, gasoline, and diesel while adding hydrogen to the products.<sup>22</sup> The upgrading technology is chosen based on the feed, type of desired product, capital cost, and operating cost. Thermal cracking yields lower conversions than hydrocracking and produces more undesirable products, such as coke. The absence of hydrogen in thermal cracking leads to more unsaturated and aromatic compounds that may require further processing. In hydrocracking the products are more desirable, but a large amount of energy is needed during regeneration of the catalyst. Upgrading by either method is a high energy and GHG emission-intensive process.<sup>23,24</sup>

### 1.3. Application of plasma processing technology for heavy oil upgrading

To reduce GHG emissions while expanding unconventional oil production, new technologies need to be developed. One developing technology uses electrical discharge plasmas to perform upgrading similar to that of an FCC.<sup>25</sup> Plasma processing of fossil fuels and biomass is an alternative emerging fuel processing technology with significant benefits compared to traditional catalytic thermal cracking.<sup>26</sup> Generally, traditional thermal and catalytic cracking methods of refining are efficient only at large scales and are not easily adaptable to changing needs and market demands.<sup>27</sup> Oil refining and upgrading using plasma instead of heat and catalysts are gaining attention as an alternative to traditional upgraders<sup>28–32</sup> such as the FCC and hydrocrackers, due to



their production of similar products with significantly less GHG emissions. Conventional upgraders have numerous challenges, including high capital costs, an intensive environmental impact, followed by catalyst deactivation through poisoning from contaminants such as sulfur and metals.<sup>33,34</sup> Electrification can help reduce the environmental impact by offsetting some of the energy consumption requirement of burning flue gas to heat furnaces and keep reactors at high temperatures and significantly reduce GHG emissions, compared to traditional oil processing methods.<sup>35–40</sup>

Plasma consists of ionized gas, enabling free ions and electrons to interact with the gas and liquid to induce chemistry.<sup>41</sup> Plasma can be artificially generated at a small scale by heating or subjecting a neutral gas to a strong electromagnetic field where the ionized gaseous medium becomes increasingly electrically conductive.<sup>42,43</sup> Some researchers have reported the results of their studies on plasma-induced heavy hydrocarbon cracking. Khani *et al.* surveyed plasma cracking of *n*-hexadecane to both lighter and heavier hydrocarbons in a batch dielectric barrier discharge (DBD) reactor with an AC power supply.<sup>44</sup> The maximum reported conversion during the process was 9.41%. Prieto *et al.* focused on plasma cracking of heavy oil to produce gaseous hydrocarbons and hydrogen.<sup>45</sup> Jahanmiri *et al.* used a nanosecond DBD plasma reactor to crack naphtha and studied the effect of the applied voltage, pulse repetition frequency, and electrode material used.<sup>46</sup> Khani *et al.* also studied the feasibility of utilizing plasma (DBD reactor) for cracking different hydrocarbons (*n*-hexadecane, lubricating oil, and heavy oil) and obtained a conversion of 6.55%.<sup>47</sup> Researchers from Japan, Matsui *et al.*,<sup>48</sup> used a plasma reactor with aluminum and copper chips to catalytically reform liquid phase hydrocarbon fuels to gas and solid phases. Rathore *et al.*<sup>49</sup> used a micro ball plasma reactor to process JP-8 liquid and convert it into lighter fuels using low energy per pulse. Wang *et al.* developed an electrical method using nanosecond pulsed multiphase plasma to convert fossil fuels at ambient temperature.<sup>50</sup> Wang *et al.* also investigated the role of bubble and impurity dynamics in the electrical breakdown and the relative breakdown voltage and energy deposition in the liquid and gas phase of multiphase hydrocarbon plasmas, for in-depth research on hydrocarbon conversion using plasmas.<sup>51,52</sup> While researchers have invented different novel plasma processing technologies for heavy oil upgrading, research on the impact of plasma processing technologies in terms of energy consumption and greenhouse gas emissions, compared to traditional catalytic thermal cracking technologies is non-existent. An LCA has also never been performed for comparing these two technologies and how they fit into the entire oil and gas industry, making this paper a first in the literature. The results of Wang<sup>7</sup> are the most efficient conversions reported and are used as the basis for the LCA.

## 2. Objectives and the scope of this LCA

The primary goals of this paper are as follows:

- Evaluate the energy consumption and GHG emissions of a TMR with WTI as the crude oil input.

- Evaluate the energy consumption and GHG emissions of a medium refinery with PPT replacing the FCC with WTI as the crude oil input.
- Evaluate the energy consumption and GHG emissions of a TDR with LLB as a crude oil input.
- Evaluate the energy consumption and GHG emissions of a traditional refinery with PPT replacing the FCC with LLB as a crude oil input.
- Complete a WTT LCA with a comparison to both traditional and plasma upgrading scenarios.
- Evaluate the energy cost of the different traditional and plasma refining configuration scenarios.
- Conduct a sensitivity analysis of the input parameters in plasma upgrading scenarios for reducing the cost difference with BAU.

## 3. Methodology

The refinery is modeled using a petroleum refinery model called petroleum refinery life cycle inventory model (PRELIM). The PPT within the refinery is modeled based upon extrapolation of the published bench scale experimental results. Energy and mass flow are calculated through the PRELIM model. GHG emissions are based upon the energy source. The lower heating value of fuels was used to calculate the associated energy content. Energies are presented as MJ per barrel, and mass flows within the refinery, in kg per day or metric ton per day. GHG emissions have been investigated with a kg CO<sub>2eq</sub> per barrel of crude as a functional unit.

### 3.1. Relationship between conversion and specific input in an oil treatment reactor

To meet the industrial demand and specifications, new technology and devices developed in the laboratory often need to be scaled up to the industrial scale, *e.g.*, to increase the production rate. Before proceeding from a laboratory scale to a full-scale commercial unit, additional investigations are required to ensure that the large-scale unit is still able to produce the results produced in the lab. The FCC has a conversion of 79.8% in the PRELIM model and the conversion is defined as reactants converted to desired products which are gas (3.3%), LPG C4 (5%), gasoline (51.5%), and LCO (20%) at 2200 kJ kg<sup>-1</sup>. Slurry oil and coke are not considered as desired products and hence not included in conversion. Considering a similar product range, the conversion for PPT is 11.7% defined as reactants converted to desired products which are hydrogen (0.27%), C2–C4 (5.8%), and C5–C15 (5.6%) at 500 kJ kg<sup>-1</sup> from hexadecane, which is a lighter feed than typical in an FCC, as explained in detail in Wang *et al.*<sup>7</sup> Extrapolating it would take about 4000 kJ kg<sup>-1</sup> in the PPT to achieve conversion to lighter products similar to that produced in FCC. While not identical to an FCC, they are similar, making it useful for the analysis of how scaled PPT could impact refinery operations.

Wang *et al.*<sup>7</sup> demonstrated conversion using specific energy inputs (SEI) from 250 kJ kg<sup>-1</sup> to 750 kJ kg<sup>-1</sup>. Additional experiments were performed to extend that data set to a SEI more



comparable with existing refinery processing technology. These experiments were performed using the same setup and methodology as presented in Wang's paper, repeating the  $500 \text{ kJ kg}^{-1}$  condition, and adding a  $2000 \text{ kJ kg}^{-1}$  data point by operating the reactor for approximately 12 hours. Fig. 1 presents the new experimental results alongside Wang's prior results showing linear performance up to  $2000 \text{ kJ kg}^{-1}$  with an  $R^2$  value of 0.98 and extrapolated to  $4000 \text{ kJ kg}^{-1}$ . Conversion to desired products is presented here, which is calculated from the measurement mass of evaporated products. Evaporated mass corresponds to on average about 83.2% of the conversion to the desired products. The new experiments measured a mass of evaporated products at  $500$  and  $2000 \text{ kJ kg}^{-1}$  of 9.81%, 33.0%, respectively. In Fig. 1, this is presented as overall conversion using the same factor of 83.2%. The  $2000 \text{ kJ kg}^{-1}$  gives more confidence on the assumption of linearity beyond what was present in Wang. The underlying reasons why this linearity is observed include: (1) most light products separate from the feedstock. This is because the reactor is maintained at  $100^\circ\text{C}$  and lighter products in the range of C1–C6+ will boil off from the reactor. As a result, the bulk of the oil still being processed will be heavy oil. (2) To quantify the above point, the liquid phase experiences a relatively minor change (5.7% at  $2000 \text{ kJ kg}^{-1}$ ) with a long residence time in the reactor as the ratio of conversion of light product to heavy product is roughly 8 : 1. Since the lighter products will be separated, the linear performance of the liquid being treated continuously is valid, as the bulk of the heavy oil is relatively unchanged and can be considered as new oil.

As shown by Wang *et al.* light and heavy products are produced and are initiated by an inherently random chain scission mechanism. Although random in initiation, the PPT selectively produces more light than heavy products. A fluid catalytic converter in a refinery, although different in mechanism, also produces both light and heavy products. In an FCC typically 79.8% of the feed is converted and 16.7% of the product is new heavy species. In the PPT at an extrapolated

79.8% conversion, Wang's results would predict 17.4% of the product as new heavy species. Thus, the plasma-induced non-thermal conversion of the liquid phase to intermediate products has a similar product distribution to that of thermal/catalytic methods utilized in the energy industry. The selectivity is thus similar in an FCC and PPT. In general, however, the selectivity of plasma processes is not as well understood as those of catalysts. Highly non-equilibrium processes are used as control knobs in PPT but are still limited by laws of thermodynamics. The cost of converting hexadecane was 12 eV per molecule as shown by Wang *et al.*<sup>7</sup> which is lower than that in most literature reported. The carbon–carbon bond energy is 3.6 eV, and the entire plasma chemistry efficiency, which includes ionization, radical production, chain reaction, thermally induced chemistry, *etc.*, is roughly 30% ( $3.6 \text{ eV}/12 \text{ eV} = 30\%$ ). The electrical efficiency of the plasma generation is also considered to be 85% to account for any losses in the electrical conversion to high voltage. A  $4000 \text{ kJ kg}^{-1}$  plasma input power would thus require about  $4700 \text{ kJ kg}^{-1}$  from the electrical grid.

### 3.2. Plasma processing technology modeling

The PPT used here to analyze the benefits of reduced GHG emissions and intensive hydrocarbon conversion is based on the paper of Wang *et al.* titled "Electric fuel conversion with hydrogen production by multiphase plasma at ambient pressure" where the researchers used a nanosecond pulsed electrical discharge PPT to partially upgrade *n*-hexadecane with methane and hydrogen at ambient pressure.<sup>7</sup> Pure *n*-hexadecane as an illustrative surrogate was treated to quantify the pathways of vapor, condensate, liquid, and residue mass conversion. Using a  $500 \text{ kJ kg}^{-1}$  *n*-hexadecane SEI ( $\sim 1\%$  of *n*-hexadecane's energy content and  $<\$1$  per barrel in electrical input cost) this plasma process converts 9.36% of the *n*-hexadecane and 20% of the methane by mass resulting in 11.7% of conversion to desired products similar in composition to that by FCC. This oil conversion process has high energy efficiency and significantly lower GHG emissions than traditional

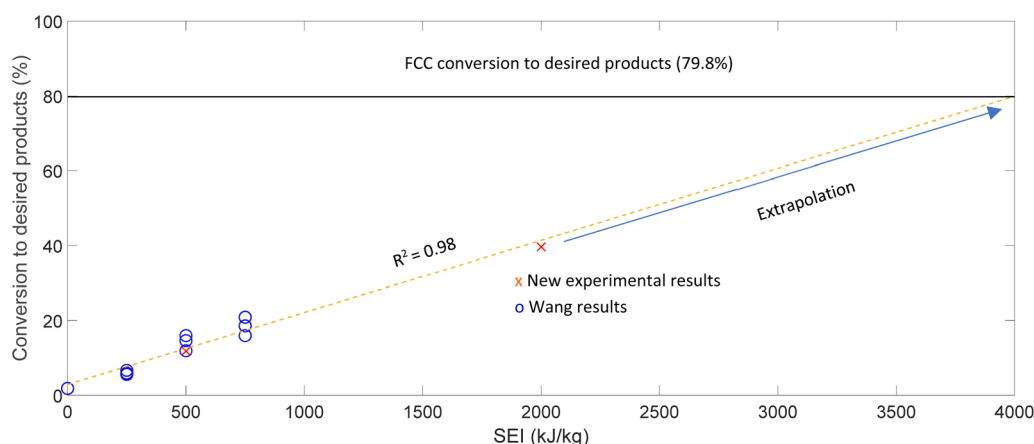


Fig. 1 SEI vs. overall conversion with new experimental results alongside Wang's prior results showing linear performance up to  $2000 \text{ kJ kg}^{-1}$  and extrapolated to  $4000 \text{ kJ kg}^{-1}$ . In an FCC, typically 79.8% of the feed is converted and the projected overall conversion for  $4000 \text{ kJ kg}^{-1}$  is similar to that of FCC.



technologies. Intimate plasma gas–liquid interactions enable high conversion and efficiency at a small scale which is very attractive for modular scale-up and integration with distributed renewable energy grids. Modeling the scaleup of this reactor to the refinery scale is based upon a multiplicity of small reactors.<sup>53</sup> Plasma processing reactors are amenable to a method of process intensification<sup>54</sup> wherein the individual micro-scale reactor is highly efficient and large-scale efficiency is obtained by linear scaling of the reactions by having thousands of reactors. This maintains the conversion and efficiency of the small-scale reactor. The near ambient pressure operating conditions allow for this to be performed without excessive capital cost.

### 3.3. Approach used to integrate the PPT into the PRELIM model

- The additional electrical energy requirements of the PPT are sourced from 100% renewable energy to power. This is done to emphasize the largest GHG impact of electrifying this refinery process.
  - The electrical efficiency to generate the plasma *via* a high voltage power system is 85%.
  - Methane and refinery fuel gas (RFG) from plasma processing is neither combusted nor emitted into the atmosphere but instead reused and recycled in a closed-loop design after hydrogen separation.
  - The pump, compressor, and other electrical requirements of the FCC and PPT are assumed to be the same. The PPT does not require high pressure operation like the FCC, that energy is instead assumed to be used for hydrogen separation. The mass flow of hydrogen is significantly lower than the mass flow of oil. The energy use for hydrogen separation is thus overestimated and will over report this small contribution of emissions from the PPT. This small inaccuracy was acceptable to simplify the problem.
  - Consistent with the other components of the refinery there is no cogeneration by combustion of coproducts for electricity generation.
  - The reported total conversion of the PPT to lighter products is 11.7%, with an SEI of  $0.5 \text{ MJ kg}^{-1}$ .<sup>7</sup> To match the FCC conversion of 79.8%, a  $\sim 4 \text{ MJ kg}^{-1}$  SEI is required for the PPT according to the linear scaleup model.
  - The output liquid lighter products are the same for the FCC and the PPT; only the cracking mechanism for conversion is different. This assumption is based on results<sup>7</sup> from Wang *et al.* showing generation of lighter end products. This assumption simplifies the comparative analysis greatly, within the existing simplifications of the PRELIM model, and within the constraints of available experimental data on PPT products on processing of VGO.
  - The output heavy end products of the PPT are higher than those of the FCC in an amount equivalent to the coke burn off in the FCC. This is higher than the measured production of heavy oil by the PPT, but again greatly simplifies the analysis.
  - Plasma-induced non-thermal conversion of the liquid phase to intermediate products has a similar product distribution to that of thermal/catalytic methods utilized in an FCC.

### 3.4. Prelim model

The Petroleum Refinery Life Cycle Inventory Model (PRELIM) is a free Microsoft Excel-based model developed by the University of Calgary that estimates energy use and GHG emissions associated with petroleum refining using unique crude oil assays.<sup>55,56</sup> PRELIM quantifies the crude oil refining energy use and GHG emissions with detail and transparency. The results are presented by product type based on chemical and rheological properties from the associated crude oil assay. Additionally, results are shown from two types of refineries where one is using only a coker and the other only a hydrocracker. The PRELIM model simultaneously calculates energy and emissions for these two different refinery types: a coking refinery and a hydrocracking refinery.

In our paper, we focus on the coking type refinery (due to the nature of the market demand in the US and especially within Canadian provinces). The GHG emissions in the BAU case are modeled and calculated using WTI which is a high API (40.8) light oil and LLB which is a Canadian heavy crude oil with a low API (18.4). The main process units are shown with their modeled configurations as used in this study in Fig. 2 through Fig. 5. Table 1 shows the corresponding inputs used for the PRELIM model. The user can select the initial conditions, the crude oil type (based on available crude oil assays), type of refinery, processing units available, and commercial fuel products to model a mass balance and GHG emissions at each processing unit in the refinery. The PRELIM model is used for the BAU flow chart to compute a mass balance and GHG emissions and these results are then compared to modeled results from PPT running the crude oil-based laboratory experimental results. This comparative analysis aims to take the same BAU process and replace only the FCC stage with PPT to investigate whether PPT is a greener solution for refining crude oil to commercial-grade fuels. Implementation of PPT in other units of the refinery is also a possible scenario but is beyond the scope of this paper.

In this paper, both medium and deep refinery configurations have been explored. For a medium conversion refinery, WTI was taken as the crude oil input because smaller refineries usually refine crude oils with a higher API while deep refineries can intake unconventional heavier crude oils as their input feed. Hence, LLB was selected as the crude oil input for the a deep configuration refinery. Fig. 2 through 5 show the process unit configurations in medium, and deep conversions. To be clear, PPT refers to the upgrading and cracking unit analogous to the FCC whereas PMR and PDR refer to the entire medium and deep configuration refineries.

### 3.5. Refining configuration

A refinery's main function is to separate heavy and light hydrocarbons in crude oil to produce commercial fuels and chemicals.<sup>46</sup> Traditional catalytic thermal cracking and hydro-treating methods convert hydrocarbons to fuels and chemicals. Fig. 2 through 5 depicts the various steps that crude oil goes through. Coker and hydrocracker are additional steps in the deep refineries. In the plasma versions of the medium and deep refineries, the FCC is replaced by the PPT.



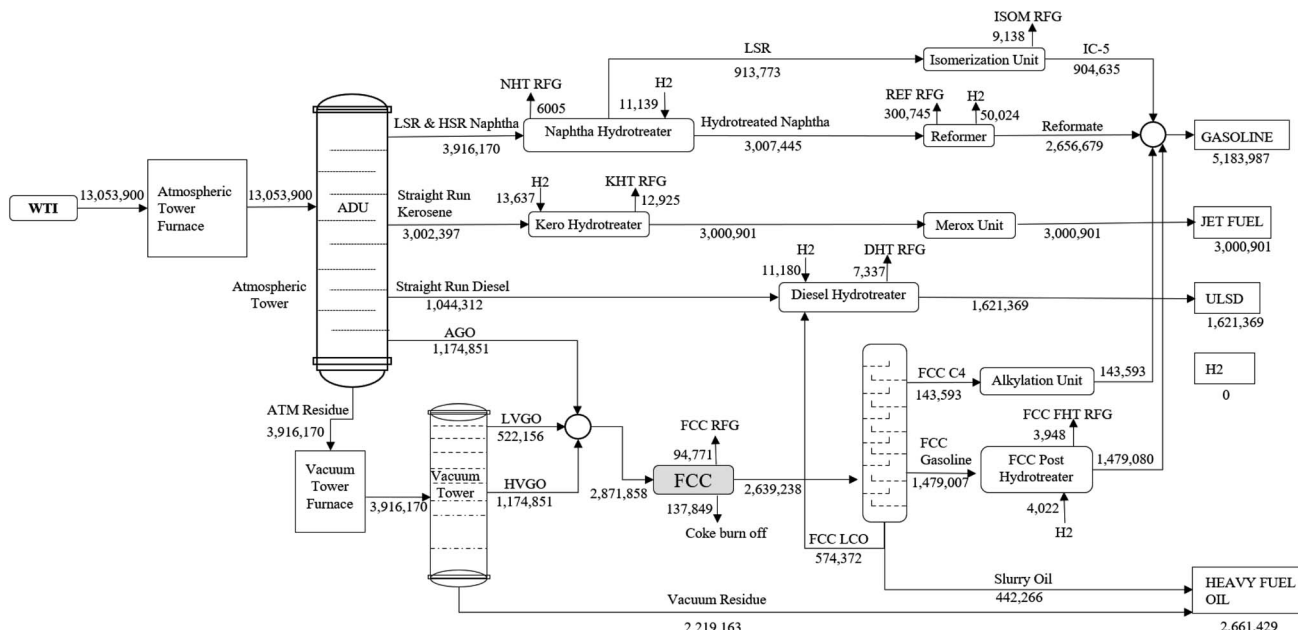


**Fig. 2** Process mass flow in a traditional medium configuration refinery. The figure includes all the processes a crude oil undergoes to turn into commercial-grade fuels. The mass flow is also displayed for each process unit and all mass balances are shown in kg per day. This configuration mainly consists of an FCC as the upgrader. The final products are gasoline, jet fuel, ULSD, heavy fuel oil, and RFG that are reused for heating in the refinery.

**Table 1** Prelim input model configuration

Option	Setting
Coking refinery	Case 1: medium conversion: FCC Case 2: deep conversion: FCC & GO-HC
Naphtha catalytic reformer option	Straight run naphtha
FCC hydrotreater option	Post-FCC gasoline hydrotreater
Electricity source	NG-fired power plant for BAU
SMR hydrogen purification option	Pressure swing adsorption
Heating value	Lower heating values
Global warming potential value	2013 IPCC AR5 (100 years)
Upstream release	Included
Off-site managed waste release	Included
Asphalt production	Minimal (0%)
Off gas product production	Minimal (0%)
Cogeneration unit	Minimal (0%)

An atmospheric tower furnace first heats filtered and desalinated crude oil to 280–350 °C. The mixture exits the furnace and enters an atmospheric distillation unit (ADU) for separation. Steam injection lowers hydrocarbon partial pressures, while recirculation pumps improve distillation efficiency. Incondensable gases will exit the tower and may be polymerized and alkylated into products or burned as heating fuel. The ADU's atmospheric gas oil (AGO) and atmospheric tower bottom (ATB) crude oils are made up of heavier hydrocarbon molecules. The AGO stream is fed to a gas oil hydrocracker to crack the liquid mixture into mostly diesel range molecules. The ATB enters the vacuum distillation unit (VDU), which operates at around 5 kPa.

and 400 °C, and uses steam and recirculation pumps to distill it. The VDU's main interval streams are light and heavy vacuum gas oil (LVGO and HVGO), and vacuum tower bottom residuum (VTB). The LVGO can be sent to the AGO hydrocracker, where the heavier cuts of LVGO and HVGO are fed into the FCC. The gas and liquid products from thermal cracking are then fractionated, with butane and lighter components going to the same polymerization and alkylation units as the incondensable gases from the ADU, gasoline going to a hydrotreater and sweetened, and diesel going to the same diesel hydrotreater as the mid-heavy distillates from the ADU, resulting in various commercial grade fuels. To induce thermal cracking, the VTB is heated to nearly 500°. The mixture is then injected with steam into the coker to reduce partial pressure. Thermal cracking produces coker gas, coker naphtha, coker gas oil (CGO), and solid carbon coke. For gasoline, coker naphtha is fed into a coker naphtha hydrotreater; then catalytic reformer, and CGO is fed into a gas oil hydrotreater and then FCC. In PRELIM, a steam methane reformer (SMR) unit was considered to produce additional hydrogen in addition to that produced as a by-product of the naphtha catalytic reformer. Hydrogen must be separated from the other steam methane reforming products. Pressure swing adsorption (PSA) has been used for hydrogen purification.

Fig. 2 shows the processing diagram for a traditional medium conversion FCC refinery that the PRELIM can model for a known crude oil assay and database factors such as heating values, global warming potential values, electricity sources, *etc.* Each processing unit stage shows the associated mass at that stage and its composition type. Fig. 3 shows the processing diagram for a medium conversion refinery with PPT replacing

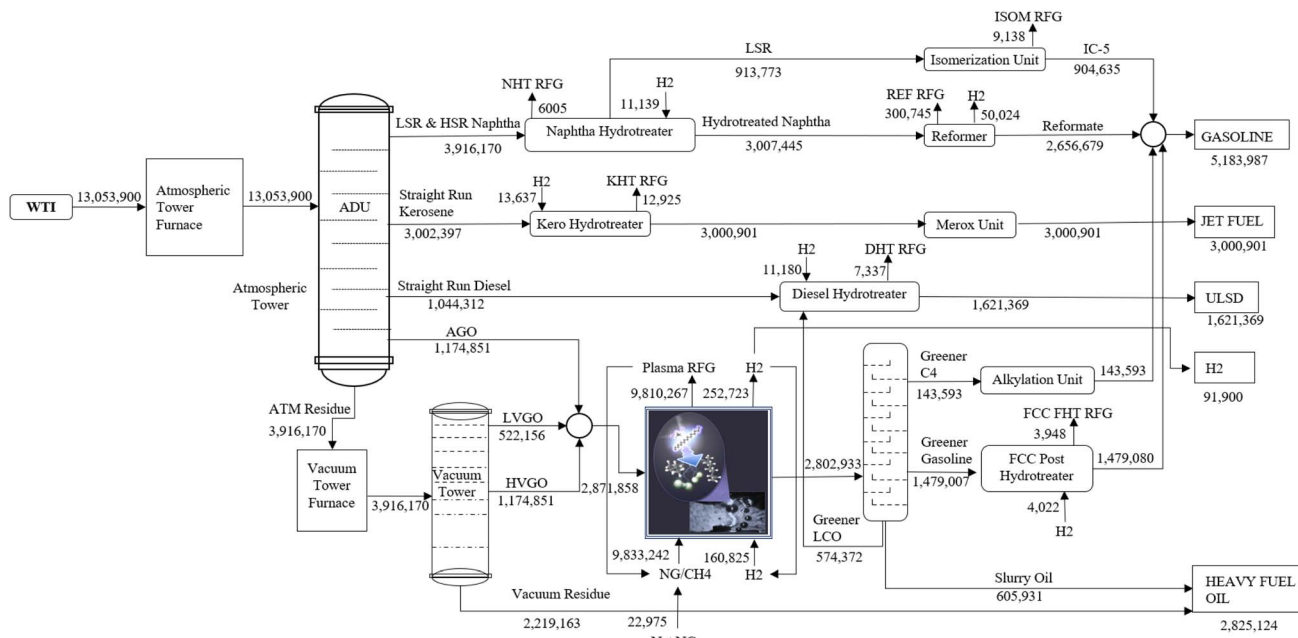


Fig. 3 Process mass flow in a plasma medium configuration refinery. This configuration mainly consists of a PPT as the upgrader replacing the FCC in BAU. All units are in kg per day.

the FCC only. The GHG emissions and energy consumption will be investigated on the FCC for a medium conversion refinery, and then after replacing the FCC with PPT.

Fig. 4 shows the processing diagram for a traditional deep conversion FCC and gas oil hydrocracker (GO-HC) coking 100 000 bbl per day capacity refinery. The GHG emissions and

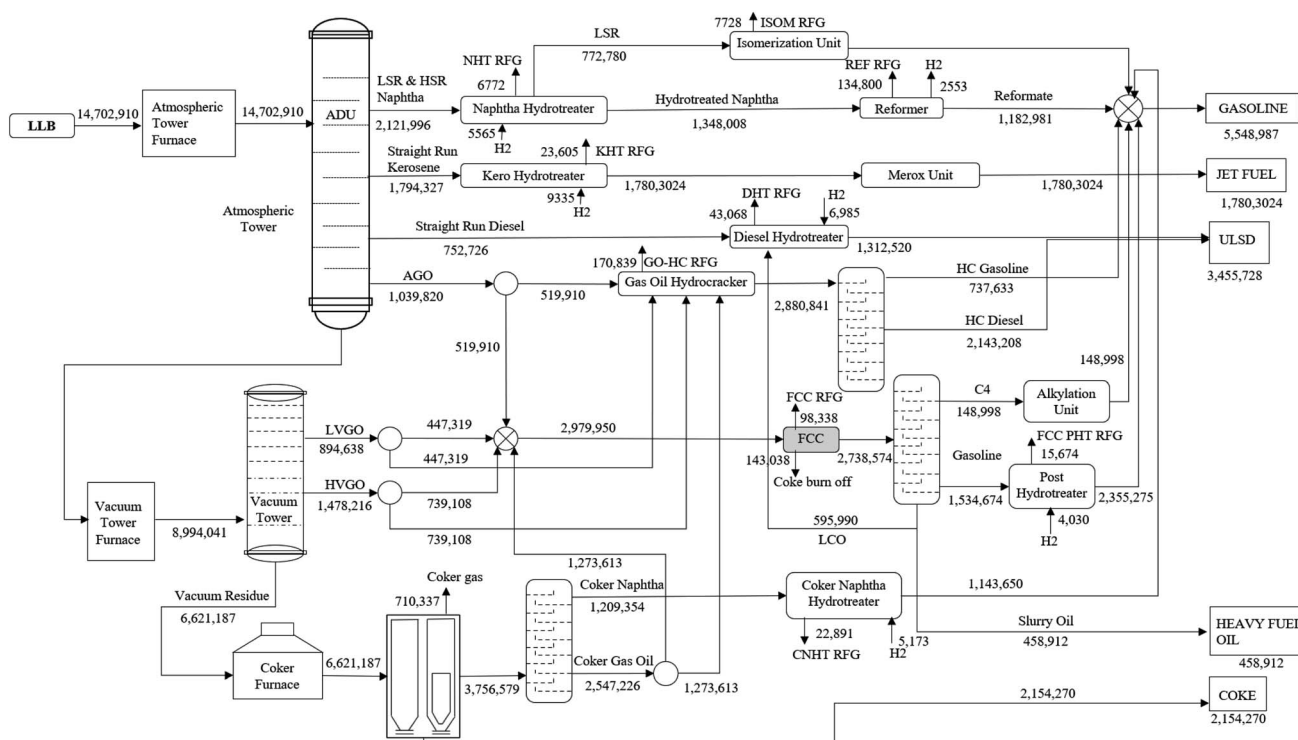


Fig. 4 Process mass flow in a traditional deep configuration refinery. The figure includes all the processes a crude oil undergoes to turn into commercial-grade fuels. The mass flow is also displayed for each process unit and all mass balances are shown in kg per day. This configuration is suitable for processing heavy crude oils and is composed of multiple upgraders and hydrotreaters such as a coker, FCC, and a hydrocracker. The final products are gasoline, jet fuel, ULSD, heavy fuel oil, coke, and RFG that are reused for heating in the refinery.

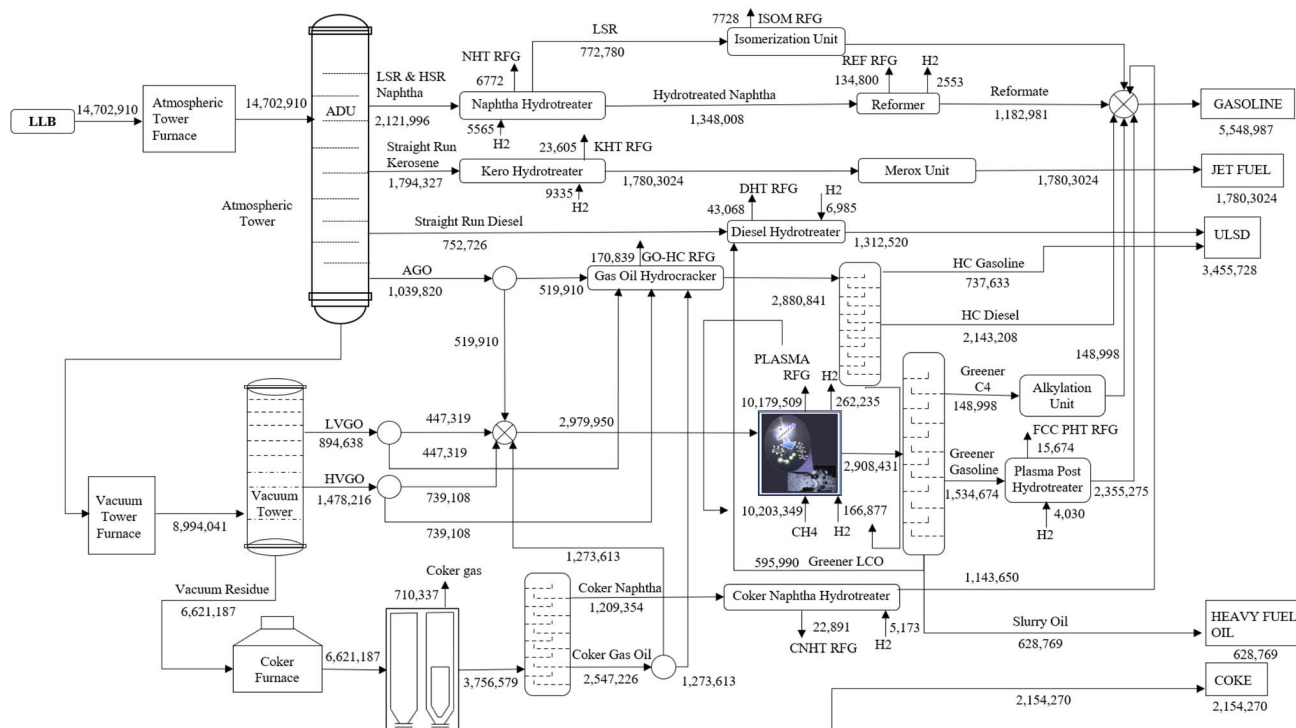


Fig. 5 Process mass flow diagram for a traditional deep conversion FCC and GO-HC coking 100 000 bbl per day capacity refinery with the FCC replaced by PPT. In this configuration, the FCC is also replaced by the PPT but the coker and hydrotreater remain unchanged.

energy consumption will be investigated on the FCC for this second scenario refinery, and then after replacing the FCC with PPT while running a comparative analysis. The difference between the TMR and TDR is that the TDR includes a coker, a coker naphtha hydrotreater, and GO-HC.

#### 4. Results and discussion

Table 2 details the process energy input and output in MJ per day for a TMR with WTI as the crude oil input. Table 3 details the process life cycle GHG emissions in metric ton  $\text{CO}_{2\text{eq}}$  per day for TMR with WTI as the crude oil input. Similarly, Table 4 details the process energy input and output in MJ per day for a TDR with LLB as the crude oil input, and Table 5 details the process life cycle GHG emissions in metric ton  $\text{CO}_{2\text{eq}}$  per day for TDR with LLB as the crude oil input. They summarize the PRELIM model processing energy inputs and outputs for an approximately 100 000 bbl per day capacity refinery. Each stage is modeled for power consumption, total gas requirement, total steam requirement, total hydrogen requirement, total RFG for onsite use, hydrogen production, and coke burn-off to quantify a mass and energy balance. The TDR is also equipped with a GO-HC and coker compared to the TMR which is only equipped with an FCC. Electrical power requirements are expressed in units of MJ per day and are referred to as the power requirement. The gas used for heating is also expressed in units of MJ per day and is referred to as the energy requirement. Steam and hydrogen use are expressed in both mass flow (ton per day or kg per day) and energy units (MJ per day).

For the TMR, as shown in Table 2, the overall major energy consumption (which is the gas consumption for providing heat) comes from the catalytic naphtha reformer requiring 7.86 TJ per day followed by the atmospheric tower requiring 4.67 TJ per day. The total gas requirement stands at 28.3 TJ per day in the TMR while the total RFG produced for onsite use is 19.6 TJ per day. Hence, in a steady-state, 8.7 TJ per day of energy needs to be supplied by burning out-sourced natural gas mainly. The isomerization unit requires the largest mass flow of hydrogen gas at 15 metric ton per day and energy consumption of 1.92 TJ per day while the total hydrogen requirement is 7.25 TJ per day with most of it being used by the hydrotreaters and isomerization unit. In the TMR, the largest power requirement is by the atmospheric tower at 90 MW h per day or 0.32 TJ per day respectively. For the outputs, the overall major energy release in the form of RFG comes from the catalytic naphtha reformer at 14 TJ per day followed by the FCC from coke burn off and total RFG for onsite use at a total of 19.6 TJ per day. The catalytic naphtha reformer produces the largest mass flow of hydrogen gas at 50 metric ton per day with an energy content of 6.35 TJ per day and is the only source of hydrogen production for the TMR. Coke burn off from the FCC releases an energy equivalent of 4 TJ per day.

The burden and offsets of GHG emissions are shown in Table 3 with units of metric ton  $\text{CO}_{2\text{eq}}$  per day for the various processing units and their associated categories of origin. The categories of origin for GHG emissions that are a burden include power requirement, net natural gas requirement, RFG requirement, total steam requirement, coke burn off, and total

Table 2 Process energy inputs and outputs – TMR – West Texas intermediate

Process unit	Input				Output			
	Power requirement	Gas requirement	Steam requirement		Hydrogen requirement		RFG for onsite use	
			MJ per day	MJ per day	kg per day	MJ per day	kg per day	MJ per day
Desalter	5387		4 676 470	219 533	714 686			
Atmospheric tower and furnace	323 200		992 102					
Vacuum tower and furnace	29 402		3 964 585	91 053	296 423	11 696	1 486 007	6005
Naphtha hydrotreater	270 997		3 632 957	83 437	271 628	14 319	1 819 347	6005
Kerosene hydrotreater	248 329							278 650
Kerosene metox unit	8287							278 443
Diesel hydrotreater	128 553		1 885 066	43 294	140 942	11 739	1 491 514	3237
Fluid catalytic cracking post hydrotreater	90 512		1 319 974	34 213	111 380	4223	536 526	2958
Fluid catalytic cracker	51 577 <sup>a</sup>		2 149 038					150 117
Fluid catalytic cracker main fractionator	34 054			9776	31 827			137 279
Alkylation unit	21 433		105 817	344 201	1 120 539			
Catalytic naphtha reformer	273 180		7 867 633					
Isomerization unit	30 076		1 729 681					
Fuel gas treatment and sulfur recovery	7635		103 964	(28 985)	(94 360)	15 137	1 923 261	300 745
Summation of process units	1 522 921		28 321 470	902 340	2 937 550	57 113	7 256 656	14 054 905
Net total	1 522 921		8 650 453	902 340	2 937 550	7091	900 977	421 048
								19 671 017
								50 022
								6 355 678
								137 849
								137 849
								4 067 283
								4 067 283

<sup>a</sup> Values that change when substituting the PPT for the FCC.

Table 3 Process life cycle GHG emissions TMR – West Texas intermediate



Table 4 Process energy inputs and outputs – TDR – Lloydminster blend crude oil

Process unit	Input				Output			
	Gas requirement		Steam requirement		Hydrogen requirement		RFG for onsite use	
	MJ per day	MJ per day	kg per day	MJ per day	kg per day	MJ per day	kg per day	MJ per day
Desalter	5402							
Atmospheric tower	324 113	6 228 841	319 719	1 040 838				
Vacuum tower and furnace	59 734	2 183 895	286 420	932 433				
Naphtha hydrotreater	124 233	1 817 772	41 748	133 911	5844	742 480	2698	125 316
Kerosene hydrotreater	141 396	2 068 573	47 508	154 662	9802	1 245 376	3589	166 513
Kerosene merox unit	4915							
Gas oil hydrocracker	457 528	2 095 128						
Gas oil hydrocracker fractionator	129 732		539 947	1 757 787	93 925	11 933 794	48 649	2 292 504
Diesel hydrotreater	103 984	1 521 251	34 938	113 740	7334	931 805	2697	125 161
Coker furnace		5 894 084						
Coker	232 661							
Coker fractionator	48 638		41 123	133 877				
Coker naphtha hydrotreater	106 690	1 560 836	35 847	116 700	5432	690 148	2419	112 325
Fluid catalytic cracking post hydrotreater	93 919	1 369 656	35 501	115 572	4232	537 739	3069	142 558
Fluid catalytic cracker	50 042 <sup>a</sup>	2 085 088 <sup>a</sup>						
Fluid catalytic cracker main fractionator	35 335		10 144	33 025				
Alkylation unit	22 240				357 452			
Catalytic naphtha reformer	124 918	3 597 668	109 800	157 394	512 394			
Isomerization unit	27 492	1 581 075			43	5415	134 801	6 313 096
Fuel gas treatment and sulfur recovery	201 960	2 749 997	(766 690)	(2 495 943)		7728	357 599	30 226
Total	2 294 995	34 753 864	893 400	2 908 448	126 611	16 086 757	868 467	40 654 552
								3 840 380
								143 038
								4 220 369 <sup>a</sup>

<sup>a</sup> Values which change when substituting the PPT for the FCC.



Table 5 Process life cycle GHG emissions TDR – Lloydminster blend crude oil

Burden				Offsets			
Power requirement	Net natural gas requirement	RFG requirement	Total steam requirement	Coke burn off	Total hydrogen requirement	RFG offsets NG upstream	Steam production
	Ton CO <sub>2</sub> eq per day						
Process unit							
Desalter	0.83						
Atmospheric tower furnace	49.80	431.03		78.33			
Vacuum tower and furnace	9.18	151.12		70.17			
Naphtha hydrotreater	19.09	117.12	7.81	10.23	60.72		
Kerosene hydrotreater	21.73	131.62	10.38	11.64	101.85		
Kerosene merox unit	0.76				—		
Gas oil hydrocracker	70.31		130.56		976.00	(1.36)	
Gas oil hydrocracker fractionator	19.94			132.29			
Diesel hydrotreater	15.98	96.61	7.80	8.56	76.21		
Coker furnace		407.86					
Coker	35.75					(189.24)	
Coker fractionator	7.48						
Coker naphtha hydrotreater	16.39	100.24	7.00	8.78	56.44		
Fluid catalytic cracking post hydrotreater	14.43	84.91	8.88	8.70	43.98		
Fluid catalytic cracker	7.69 <sup>a</sup>		129.93 <sup>a</sup>		484.71 <sup>a</sup>		
Fluid catalytic cracker main fractionator	5.43			2.49			
Alkylation unit	3.42						
Catalytic naphtha reformer	19.20		224.19		(18.69)	(314.08)	
Isomerization unit	4.22	84.66	22.28		0.44		
Fuel gas treatment and sulfur recovery	31.03	190.30				(187.84)	
Refinery level							
CO <sub>2</sub> eq per day kg per bbl	3.53 <sup>a</sup>	17.95	5.49	4.07	4.85	(1.88)	
					13.15	(3.14)	
							Total 43.70

<sup>a</sup> Values which change when substituting the PPT for the FCC.

hydrogen requirement. The categories of origin for GHG emissions that are an offset (reducing emissions) include RFG offsets, NG upstream, hydrogen production, and steam production. These are more fully described in the PRELIM documentation.<sup>55</sup> The total kg CO<sub>2eq</sub> per bbl can be shown below for each category of origin and the major GHG emitter is the net natural gas requirement emitting 11.82 kg CO<sub>2eq</sub> per bbl.

The largest GHG emitting burden is from the FCC with a total of 629-metric ton CO<sub>2eq</sub> per day followed by the naphtha hydrotreater with a total of 458-metric ton CO<sub>2eq</sub> per day. The greatest hydrogen gas-consuming processing unit is the isomerization unit with 157-metric ton CO<sub>2eq</sub> per day GHG emissions. The largest GHG emission offset is by hydrogen production by the catalytic naphtha reformer reducing 520-metric ton CO<sub>2eq</sub> per day. For this case it is labeled an offset because the SMR is not needed to produce that hydrogen. In

general, the PRELIM model uses the 'offset' label for processes which are provided by internal processes and an external source is not needed. The largest GHG emitting stage found was the FCC from the coke burn off resulting in 500 metric ton of CO<sub>2eq</sub> per day, which is about 17% of the total.

For the TDR, as shown in Tables 4 and 5, the overall major energy consumption by heating of gas comes from the atmospheric tower requiring 6.22 TJ per day followed by the coker furnace requiring 5.89 TJ per day. For the outputs, the overall major energy usage comes from the total RFG for onsite use from the coker at 27.5 TJ per day. The GO-HC requires the largest mass flow of hydrogen gas at 94 000 kg per day and an energy consumption of 11.9 TJ per day. The CNR produces the largest mass flow of hydrogen gas at 30 metric ton per day with an energy content of 3.84 TJ per day. There is a 5% mechanical loss for hydrogen consumption due to embrittlement of the walls. Thus, hydrogen consumed is more than the hydrogen

Table 6 Detailed calculations of different scenarios for FCC and PPT units

Parameter	West Texas intermediate		Lloydminster blend	
	Medium refinery: FCC	Medium refinery: plasma	Deep refinery: FCC	Deep refinery: plasma
Mass flow balance	Oil mass flow (kg per day)	2 871 858	2 871 858	2 979 950
	Oil volume flow (bpd)	20 467	20 467	19 858
	Feed API gravity	28.8	28.8	18.4
	Natural gas intake for conversion (kg per day)	—	9 833 242	10 203 349
	FCC fuel gas released (recycled for plasma) (kg per day)	94 771	9 810 267	98 338
	Net NG as the raw material (kg per day)	—	22 975	—
	H <sub>2</sub> gas released (kg per day)	—	91 899	—
	Total liquid outflow (kg per day)	2 639 238	2 802 933	2 738 574
	Coke burnoff (kg per day)	137 849	0	143 038
	Total heavy oil exiting (kg per day)	442 266	605 935	458 912
Energy requirement	Electricity [non-renewable] (MJ per day)	51 577	51 577	50 042
	Electrical efficiency of the plasma process	—	0.85	—
	Electricity [renewable] (MJ per day)	—	13 514 626	—
	Gas (MJ per day)	2 149 038	—	2 085 088
	Catalyst coke (MJ per day)	4 067 283	—	4 220 369
	SEI (MJ kg <sup>-1</sup> )	2.2	4.0	2.2
	Plasma chemical efficiency	30%	30%	4.0
	Hydrogen fuel cell efficiency	60%	NA	—
	Electricity non-renewable (ton per day)	8	8	8
	Electricity renewable (ton per day)	—	63	126
GHG emissions CO <sub>2eq</sub>	Net natural gas (ton per day)	—	—	—
	RFG (ton per day)	136.0	—	130.0
	RFG offsetting NG upstream (ton per day)	(13.0)	—	(16.0)
	Catalyst coke (ton per day)	500.0	—	485.0
	Total CO <sub>2eq</sub> emission (kg per bbl)	6.3	0.08	6.07
	Total hydrogen production (kg per day)	—	91 899	—
	The energy content of H <sub>2</sub> (MJ)	—	11 671 231	—
	Total CO <sub>2</sub> reduction by hydrogen <i>via</i> PPT (ton per day)	—	955	—
	Total CO <sub>2</sub> reduction by hydrogen <i>via</i> PPT (kg per bbl)	—	9.57	—
	Total H <sub>2</sub> required by the refinery (ton per day)	5.95	5.95	13.15
Hydrogen emission offset	Surplus CO <sub>2</sub> emission credit <i>via</i> PPT due to greener hydrogen production (kg per bbl)	—	3.62	—



required. In the TDR, the largest power requirement stage is the GO-HC at 0.46 TJ per day. The largest GHG emitting stage is the GO-HC from the total hydrogen requirement resulting in 976 metric ton of CO<sub>2eq</sub> per day. The largest energy consuming stage is the GO-HC from the total hydrogen requirement at 11.9 TJ per day while the largest mass flow rate was found at the GO-HC fractionator from the total steam requirement at 540 metric ton per day. The largest total energy consumption was found from stages with total RFG onsite usage resulting in 40.6 TJ per day. The largest total GHG emissions were found from stages with total net natural gas requirement onsite usage at 17.95 metric ton CO<sub>2eq</sub> per day.

The detailed calculations of alternate scenarios for the FCC unit and PPT unit are shown in Table 6. The first section of the table provides the mass balance of the technologies and is followed by the energy requirements. Next, GHG emissions of both the technologies are compared and finally, the hydrogen offset is evaluated. Oil mass flows into the FCC and PPT processing unit are the same with 2871 metric ton per day for the medium refinery and 2979 ton per day for the deep refinery. The API of the feedstock for the medium refinery is 28.8, while for the deep refinery it is 18.4. The PPT operates as a multiphase reactor and requires natural gas as a raw material. RFG can also be used as a raw material for the plasma reactor, assuming that the conversion will be similar and hence is recycled. Only the net mass flow difference is compensated by supplying natural gas externally. As such, the medium plasma refinery requires 23 metric ton per day while the deep plasma refinery requires 23.8 metric ton per day. Hydrogen is produced as a coproduct with the medium refinery producing 92 metric ton per day and the deep plasma refinery producing 95.3 metric ton per day. The volume outflow is different for the plasma and FCC because the FCC burns off the coke to regenerate the catalyst and provide heat. Catalyst and thermal cracking temperatures are not required in a PPT unit. The API gravity outflow is assumed to be the same, 47.7, for both configurations.

The energy required for cracking and upgrading is provided by heat in the FCC while the PPT processing unit intakes renewable energy as electricity. The upgrading mechanism and product distribution are again discussed in detail in the Wang *et al.* paper<sup>7</sup> on which these results are based. The electricity required to operate pumps, compressors, and other related components is assumed to be the same for both processing units in the medium refinery with 53 GJ per day and deep refinery requiring 63 GJ per day. Operating PPT at ambient pressure is certainly advantageous because the material requirements on the containment vessels and similar equipment are less stringent than those in high pressure operation; this can be reflected in the capital expenditures (CAPEX) and operating expenses (OPEX) compared to those of an FCC. For modelling purposes, the CAPEX and all OPEX are not incorporated to the economics as the OPEX in the model is solely based on the energy consumption. Hence, the advantages of PPT at ambient pressure are not directly reflected here. However, for seamless integration into the refinery, compression to higher pressure may be necessary and there is enough flexibility in the PPT to accommodate the energy expense without providing it

externally. Based on calculations, the energy required for H<sub>2</sub> separation is 10.51 MJ per bbl or <2% of the total energy required for processing a barrel of oil. This energy can be compensated by recovering the waste heat from PPT. The PPT has a working efficiency of 30%. The actual waste heat that can be converted to energy from 70% of 70 MJ per day energy spent on renewable energy to power PPT, is approximately 11 MJ per bbl which is enough to power the pumps and compressors needed for hydrogen separation with purity greater than 85% and other energy expenditures. This is not considering the waste heat that can be extracted from fuel cells, and hence we are maintaining a conservative estimate and leaving enough room to account for small, unexpected energy consumption that might be required to integrate the PPT with the refinery. Also, the electricity cost (non-renewable energy) of 51 577 MJ per day, similar to the FCC requirement, has also been added to PPT for any miscellaneous operations.

The total conversion of the FCC is 79.8% according to the PRELIM model considering the converted products to be gas, LPG, gasoline, and LCO. With the energy input as natural gas, steam, and burning of coke from catalyst regeneration, the SEI of the FCC is 2.2 MJ kg<sup>-1</sup>. For the PPT the reported total conversion to desired products similar in composition to those of FCC is 11.7% with an SEI of 0.5 MJ kg<sup>-1</sup>.<sup>7</sup> Plasma upgrading reactions mostly occur in the reaction zones in the region between high voltage and ground in a multiphase environment, and increasing these reaction zones is going to increase the conversion linearly. The linear relation assumption between the SEI and conversion in PPT is supported by Wang *et al.*<sup>7</sup> Thus, to match the conversion of the FCC, eight times more SEI is required in the plasma reactor bringing the SEI to 4 MJ kg<sup>-1</sup> which is 1.8 times more energy-intensive than an FCC. With the electrical efficiency of the plasma generation process assumed to be 85%, this brings the renewable energy consumption of a medium plasma processing unit to 13.5 TJ per day and the deep plasma processing unit to 14 TJ per day for approx. 100 000 bbl of crude oil. This is about 160 MW (requiring an equivalent of about 1000 acres of solar panels [8 MW per acre])<sup>57</sup> or about 0.4% of the wind turbine production in Texas.<sup>58</sup> The global warming potential (GWP) varies for different processes. Electricity generated by an NG-fired power plant has a GWP of 153.7 g CO<sub>2eq</sub> per MJ while thermal heat provided by NG and RFG combined is 58.47 g CO<sub>2eq</sub> per MJ. Heat provided by only NG is 62.27 g CO<sub>2eq</sub> per MJ. Renewable energy has a minor emission footprint of 9 g CO<sub>2eq</sub> per MJ while hydrogen produced *via* SMR is 81.8 g CO<sub>2eq</sub> per MJ. The additional hydrogen produced by the plasma reforming unit can significantly reduce GHG emissions by offsetting the hydrogen produced *via* SMR which is a tremendous GHG emitting process. The medium PPT processing unit can offset 9.57 kg CO<sub>2eq</sub> per bbl while the deep PPT processing unit offsets 9.90 kg CO<sub>2eq</sub> per bbl. There is still a surplus of hydrogen remaining in the PMR configuration due to the abundance of the gas produced during the conversion which can be used as a renewable electricity feedstock *via* a fuel cell to provide part of the renewable energy input requirement or the hydrogen can be sold to nearby processing facilities. All calculations use the lower heating values for quantifying the



energy content. In our case, for PMR, the excess hydrogen is used as a feedstock for producing electricity *via* a fuel cell with 60% efficiency.

The bar chart results shown in Fig. 6 compare the energy use and GHG emissions per barrel between PPT replacing the FCC in a traditional medium and deep refinery while comparing it to BAU. Energy use and GHG emissions are quantified using the PRELIM model and are measured from various sources: electricity, renewable energy, electricity from hydrogen using a fuel cell, heat from recycling RFG, heat from burning input natural gas, heat for steam generation, the energy required for hydrogen production *via* SMR, the energy content of hydrogen *via* electricity, the energy content of hydrogen produced *via* CNR, coke burn off, and other emissions. As shown in Fig. 6a, the plasma deep refinery was shown to require the most energy usage at 715 MJ per bbl of crude oil which is an energy increase of 14% from 626 MJ per bbl when replacing the FCC with PPT in the TDR. The TMR required 446 MJ per bbl of energy while replacing the FCC with PPT in the TMR, which increased the energy consumption by 18% to 528 MJ per bbl. The typical energy content of a barrel of oil is 6120 MJ per bbl of crude oil.<sup>59</sup> Therefore, in the case of the TDR, the energy increase is only 1.8% of the energy content of a barrel of oil. PPT requires higher energy per barrel of crude oil for the electricity input requirement based on the PRELIM model. The plasma energy input requirements and efficiency is based on the results of Wang<sup>7</sup> and may still be improved by further research in that field. In general, deep refineries also require more energy than medium refineries due to the extensive infrastructure and equipment

required to refine heavier crude oils such as the coker and hydrocracker. Fig. 6b shows that the TDR has the largest GHG emissions at 43 kg CO<sub>2</sub>eq per bbl and a GHG emission reduction of 35% was found when replacing the FCC with PPT processing in the TDR. The TMR had GHG emissions of 29 kg CO<sub>2</sub>eq per bbl and a GHG emission reduction of 21% was found when replacing the FCC with PPT in the TMR. Thus, PPT reduces emissions by up to 8.7 kg CO<sub>2</sub>eq per bbl in the deep refinery configuration and 6.5 kg CO<sub>2</sub>eq per bbl in the medium refinery configuration. In both the TMR and TDR cases, the majority of the GHG emission reduction when using PPT was due to mitigating FCC coke burn off and hydrogen production *via* SMR. Also, GHG emissions from providing heat by burning RFG and natural gas decreased because energy is provided by renewable electricity in the PPT refinery configurations. Renewable electricity has negligible emissions and powering refineries using renewable electricity is a pathway forward for reducing refinery induced GHG emissions while moving toward a net zero world in-line with the Paris Climate Accords.

The bar charts in Fig. 7 compare the cost in \$USD per barrel of crude oil between PPT replacing the FCC in a traditional medium and deep refinery, while comparing it to BAU. The costs are quantified using data from the PRELIM model with typical unit energy costs and are calculated for various sources: electricity, renewable energy, electricity from hydrogen using a fuel cell, heat from recycling RFG, heat from burning input natural gas, heat for steam generation, the energy required for hydrogen production *via* SMR, the energy content of hydrogen *via* electricity, the energy content of hydrogen produced *via*

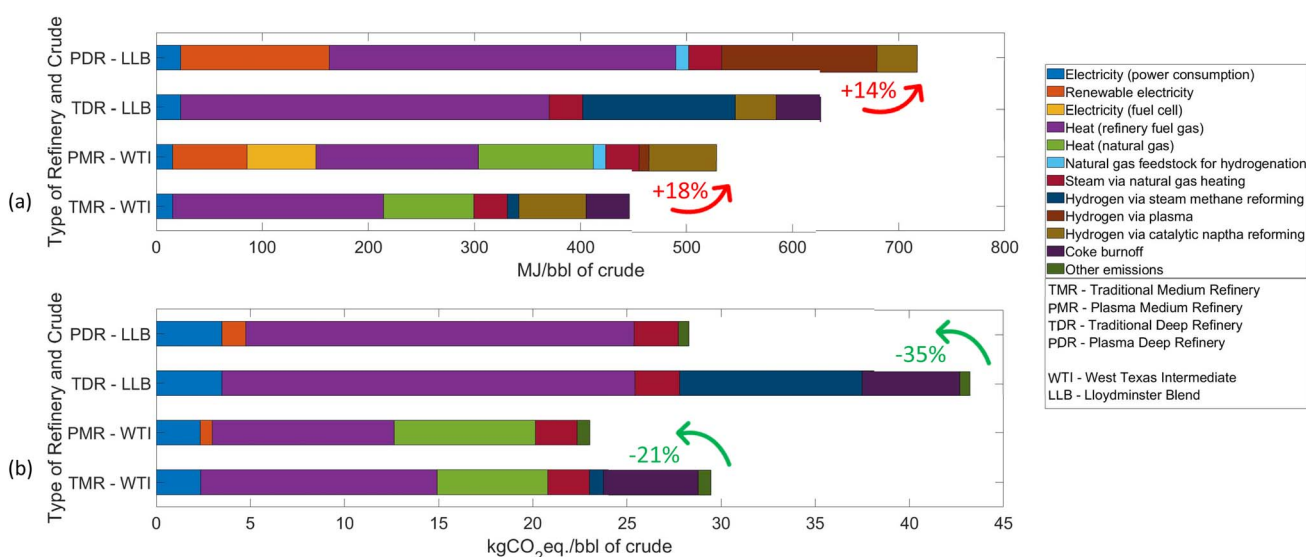


Fig. 6 (a) The energy consumption includes power in the form of electricity, renewable electricity to fuel plasma technology, electricity from a fuel cell using excess hydrogen produced, heat from RFG that is recycled, heat from natural gas, the energy content of natural gas as a feedstock in plasma technology for hydrogenation, steam production *via* natural gas heating, hydrogen production *via* steam methane reforming, hydrogen production *via* CNR, the energy released from coke burn off, and other emissions. The four different refinery configurations are TMR and PMR with WTI as the crude oil input and TDR and PDR with LLB as the crude oil input. (b) Comparison of the GHG emission from the four different refinery scenarios concerning the different energy consumption methods. Even though the plasma refinery configurations consume more energy, the results have shown that it is more environmentally friendly with less GHG emissions compared to the traditional refinery configurations. The deep refineries have more energy consumption and GHG emissions associated with them due to processing heavier crude oils.



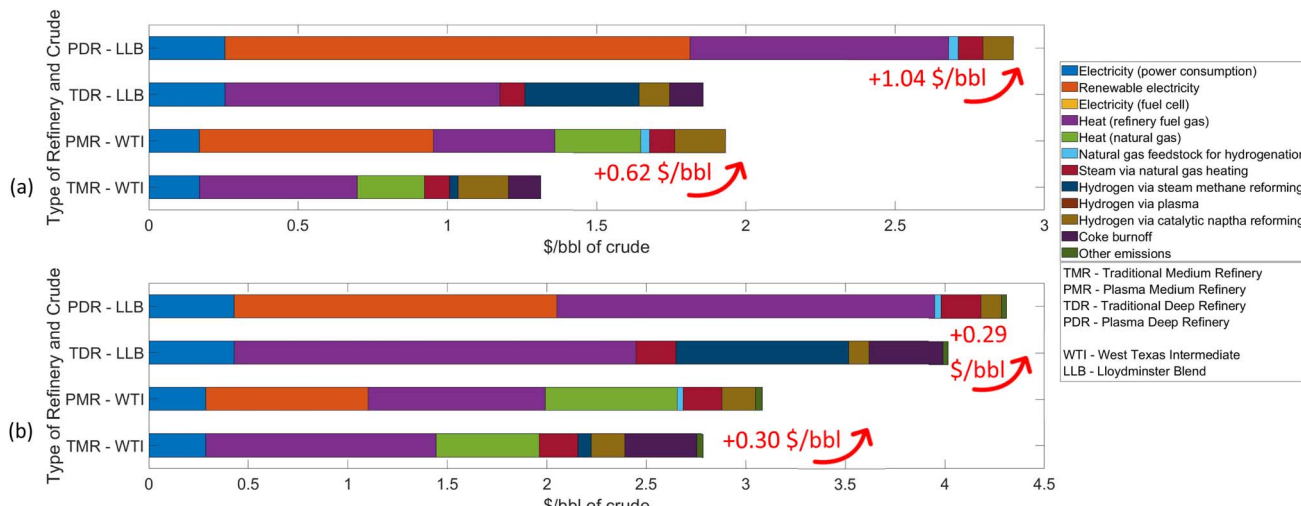


Fig. 7 (a) Comparison of energy cost with tax by using process units in different refinery scenarios. (b) Includes the carbon tax at a rate of \$0.05 per kg CO<sub>2</sub>eq from the GHG emissions in addition to the energy cost. Adding a carbon tax reduces the cost difference to 10%.

CNR, coke burn off, and other emissions. The cost of electricity from renewable energy (wind) and fossil fuels is considered to be the same at \$0.04 per kW h or \$0.011 per MJ (ref. 60 and 61) while the cost of thermal energy *via* natural gas burning is considered to be \$0.00265 per MJ.<sup>62</sup> The cost of electricity is higher than that of thermal energy in general. With increasing worldwide geopolitical pressure to reduce GHG emissions and prevent atmospheric temperatures from increasing more than 1.5 °C above pre-industrial levels, many developed countries such as Canada have implemented a carbon tax associated with emitting CO<sub>2</sub> to help mitigate climate change. Hence, a carbon tax of \$0.05 per kg was added to the cost per barrel in the traditional refinery configurations and credited back to the PPT refinery configurations. As shown in Fig. 7a, the TDR was shown to have a cost of \$1.86 per bbl of crude oil without a carbon tax and the cost increased by 59% when replacing the FCC with PPT in the TDR. However, when a carbon tax is considered, the cost of the TDR becomes \$4 per bbl and only increases by 11% with a PDR configuration as shown in Fig. 7b. This makes the PDR configuration more economically feasible in a carbon tax environment. Thus, the weight of the GHG emission cost *via* a carbon tax is significant. Similarly, in the case of the medium refinery configuration, the energy cost of the TMR is \$1.31 per bbl of crude oil and increases by 47% when replaced by PPT. However, a carbon tax reduces the difference to 10%. Thus, PPT increases the cost by only \$0.29 per bbl in the deep refinery configuration and \$0.30 per bbl in the medium refinery configuration. Note that this cost per barrel is only the cost of the energy associated with the processing, and other factors contribute to an overall refining cost of ~\$46 per bbl.<sup>63</sup> Relative to this overall refining cost, the increment due to electrical energy is only <1%. A sensitivity analysis is later performed to account for the variance in electricity costs, carbon tax, specific energy input to PPT for similar conversion to FCC, and hydrogen yield from PPT.

Another aspect to consider is the cost of energy factored into the price of oil per barrel. Customers may want to reduce their carbon footprint and be willing to purchase greener fuels at an additional cost. Such models already exist in the energy sector. For example, in Texas, consumers who want to reduce their carbon footprint have the option to purchase electricity from a renewable source at an additional cost.<sup>64</sup> While using a market price of WTI at \$85 per bbl and LLB at \$72 per bbl,<sup>65</sup> the energy cost represents a small percentage increase in the total cost per barrel as shown in Fig. 8. The TMR energy cost adds \$2.79, while the PMR adds \$3.08, for a net cost increase of only 0.33%. Similarly, the energy cost adds \$4.02 to TDR while the PDR adds \$4.31, resulting in a net cost increase of only 0.38%. Perhaps another benefit is the total amount of final product distributions. Gasoline, jet fuel, USLD, heavy end, coke, and sulfur are the end products. All refinery configurations have an input of approximately 100 000 barrels per day. In the PPT configuration

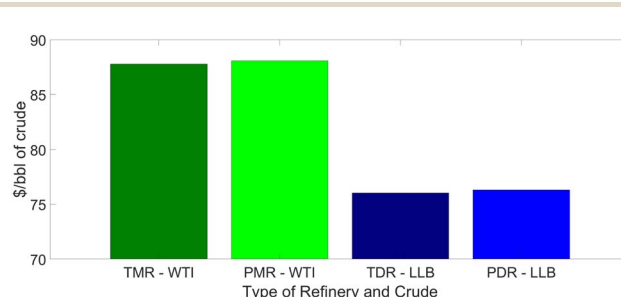


Fig. 8 Cost of energy incorporated into the cost of oil per barrel. With the cost of WTI at \$85 and the cost of the Lloyd Minster blend at \$72, the energy cost is a small percent increase in the total cost per barrel. The TMR energy cost adds \$2.79 while the PMR adds \$3.08 resulting in a net increase cost of only 0.33%. Similarly, for the TDR, the energy cost adds \$4.02 while the PDR adds \$4.31 resulting in a net increase cost of only 0.38%. All \$ values are in USD.



case, coke is a minor product output since it is not burnt to provide heat and can be added to the pool of final products.

## 5. Sensitivity analysis of PPT

A sensitivity analysis was performed on the key parameters that impact the energy cost significantly for both refinery configurations. Fig. 9 shows the results as tornado plots for both refinery configurations. The following parameters are considered: hydrogen yield from PPT, SEI, carbon tax, renewable energy cost, and a scenario where all the parameters are favorably offset. Hydrogen yields from PPT, SEI, and carbon tax were varied by  $\pm 20\%$  and the renewable energy cost was varied by 50% as several sources of renewable energy with different price ranges can be applied. In fact, with the right power purchase agreement (PPA) the cost difference can increase the profit margin of PPT significantly.<sup>66</sup> The plasma process will be impacted more since it relies on electrical energy. Low price PPAs are only negotiable when there is the ability to shut down a process relatively rapidly, as with the modular and scalable PPT demonstrated here.<sup>53</sup> The response of the cost difference between traditional and plasma refinery configurations is reported. A negative cost difference indicates that the PPT is more expensive than the traditional method whereas a positive cost difference means PPT is more economical than BAU and can be implemented without compromising profit or functionality. Increasing both hydrogen yield using PPT, and implementing a carbon tax will reduce the cost differences favoring PPT. On the other hand, increasing SEI for PPT will increase the cost difference as more energy is required to attain the same conversion as an FCC, and thus, this will favor the traditional method. For renewable energy costs, increasing the cost favors

the BAU because PPT is dependent on the cost of renewable energy. The default cost difference is  $-\$0.30$  per bbl of crude oil for the medium refinery configuration. PPT can breakeven with the traditional method and be more profitable by increasing the hydrogen yield and carbon tax, decreasing SEI, and reducing the cost of renewable energy.

Thus, if multiple scenario targets are implemented as shown by the best and worst-case scenario in the optimized parameter set, PPT can be feasibly implemented economically at an industrial level. The profit range can reach  $\$0.44$  per bbl in the medium refinery. The deep configuration refinery is more sensitive to the parameters with the difference ranging from  $-\$1.8$  to  $\$1.35$ . Similarly, in this configuration, by decreasing SEI, increasing carbon tax and hydrogen yield, and reducing the cost of renewable energy PPT can breakeven with BAU and be profitable. Thus, in certain scenarios, PPT can contribute both toward reducing GHG emissions and be a viable business model that has been shown to be feasibly profitable.

## 6. LCA: WTT analysis

An LCA was also performed for the deep refinery configuration comparing the TDR and PDR. The BAU pathway is shown in Fig. 10. The system boundary for the WTT analysis incorporates the process of extraction, transportation, mixing, refining, and product distribution. The refining configuration comparison is for BAU and PPT. The recovery and extraction processes are by steam-assisted gravity drainage (SAGD) with the condition of no cogeneration followed by transportation of the diluent at 3000 km to Canadian oil sands. The diluent is mixed with bitumen to form dilbit (diluted bitumen) which is then transported back to US refineries at 3000 km. The dilbit is then refined either as BAU

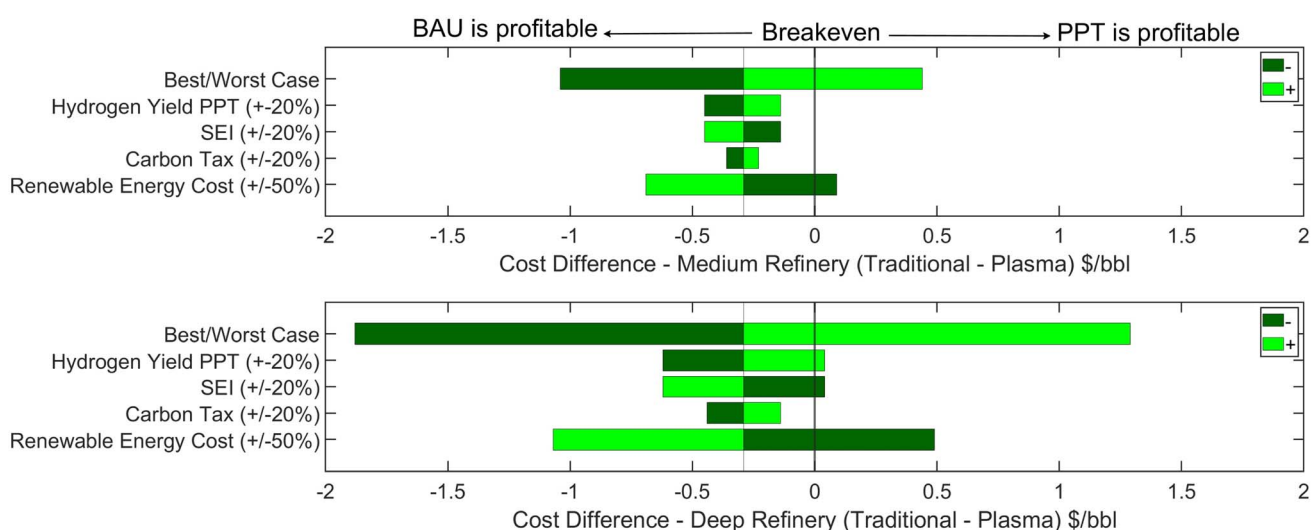


Fig. 9 Sensitivity analysis presented in tornado plots of important parameters such as plasma yield, SEI, and carbon tax affect the cost difference (traditional-plasma) \$ per bbl. When increasing the carbon tax and hydrogen yield from plasma, the PPT configuration is favored whereas increasing SEI will increase the cost difference further favoring the traditional method. An optimized scenario highlighting min and max product yields is also obtained. A negative cost difference shows that PPT is not feasible economically considering the energy cost and hence the difference needs to be reduced by optimizing the process. Renewable energy cost makes the greatest impact in price difference. Decreasing renewable energy price favors PPT significantly.



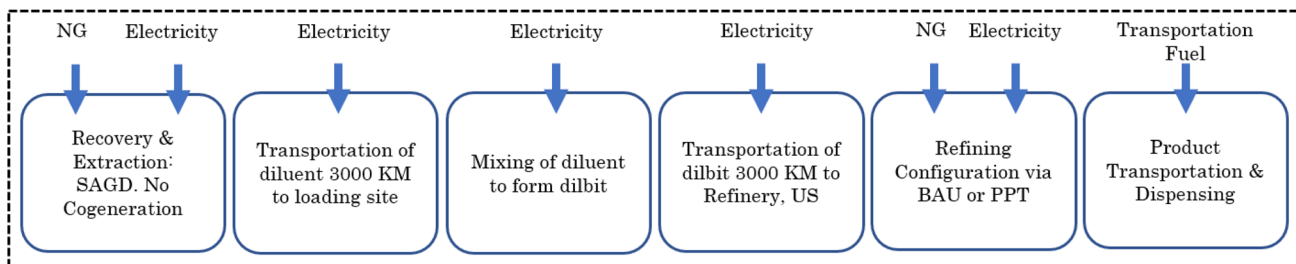


Fig. 10 System boundary for the WTT analysis incorporates the process of extraction, transportation, mixing, refining, and product distribution. The refining configuration comparison is for BAU and PPT.

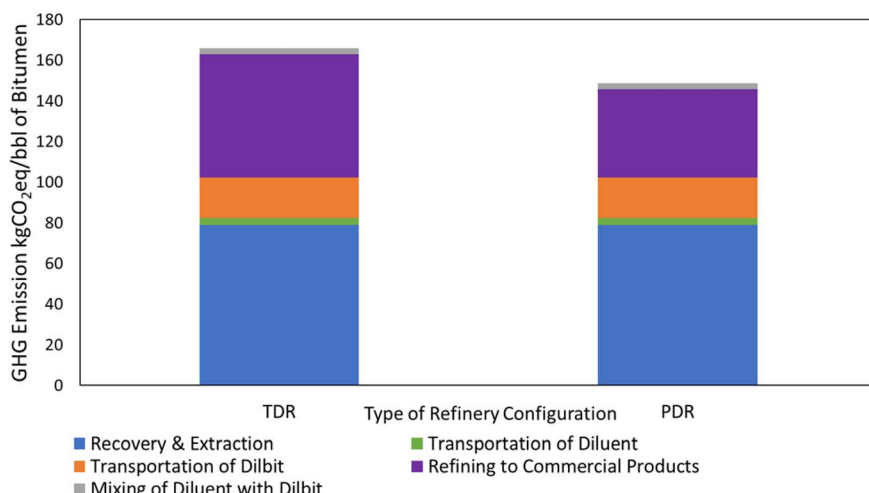


Fig. 11 WTT analysis on the deep configuration refinery. The GHG emission cycle for the TDR is 166 kg CO<sub>2</sub>eq per bbl of bitumen whereas for PDR it is 149 kg CO<sub>2</sub>eq per bbl of bitumen. This results in a GHG emission decrease of 10.3% when comparing the life cycle from WTT.

or using PPT to produce consumer products such as gasoline, diesel, jet fuel, *etc.* The products are then transported to necessary gas stations and are ready for dispense. Upon WTT analysis, as shown in Fig. 11, the GHG emission cycle for TDR is 166 kg CO<sub>2</sub>eq per bbl of bitumen whereas for PDR it is 149 kg CO<sub>2</sub>eq per bbl of bitumen.

This results in a GHG emission decrease of 10.3% when comparing the life cycle from WTT. The US consumed an average of 20.54 million barrels of crude oil.<sup>67</sup> PPT reduces emissions by up to 8.7 kg CO<sub>2</sub>eq per bbl in the deep refinery configuration. Integrating an upscaled PPT to perform just 3% of the upgrading in a refinery in the US can translate to reducing 2 million metric tons of CO<sub>2</sub>eq per year, resulting in a significant milestone toward a net zero world in-line with the Paris climate accords.

## 7. Outlook

Fossil fuels continue to be among the world's most important sources of energy, and the electrification of refineries at a large scale is difficult to achieve at a pace to help mitigate climate change. The potential of a novel technology such as plasma processing technology (PPT) in electrifying conventional refineries will lead to significantly lower GHG emission with comparable conversion, adequate energy efficiency of the process to

produce commercial grade fuels, excellent modularity, and integration with renewable electricity. PPT has the potential to replace an FCC and other upgrading technologies such as a coker, hydrocracker, *etc.* with adequate research and engineering. PPT will further reduce GHG emissions from refineries. Emerging innovations that involve reducing the emission footprint of refining fuels while capitalizing on their advantages will be an integral component of the energy transition.

At the same time, countries around the world are increasingly enacting carbon pricing initiatives such as emission trading schemes and carbon taxes as part of nationally determined contributions under the Kyoto Protocol and Paris Climate Accords. Additionally, companies within these jurisdictions are adopting ESG (environment, social, governance) mandates committing themselves to reduce emissions, typically with a net-zero carbon emission goal by 2050. While the aspirations of these countries and companies are admirable, in practice most have been unable to live up to their commitments precisely because of the difficulty of mitigating emissions. To satisfy investors who are increasingly environmentally conscious or to comply with legislation that externalizes the consequences associated with carbon emissions, companies are accelerating toward satisfying these factors and will subsequently turn to technology to ensure continual growth in the

energy transition. Various scenarios have been presented for the future of crude oil demand; however, fossil fuels will play an essential role in navigating the energy transition. As global demand levels off due to increasing carbon accountability, the greenest and cheapest barrels will increasingly be selected by the market. Reducing the environmental footprint of refining heavy oil would allow high emission intensity reserves to be produced more feasibly during the energy transition.

With a positive outlook into the future, PPT is still a newcomer in the traditional oil and gas industry that has operated for a hundred years. Like all emerging technologies that have not matured, they have advantages and disadvantages. The working mechanism of PPT under multiphase conditions is rather complex and no model has been developed to investigate it since the cracking occurs as a random chain scission event, and the selectivity of the products is not very well controlled. Hence, it is rather difficult to precisely control the chemistry of the products. Furthermore, additional safety measures are required for plasma generation as it is carried out using high voltages. There is also a significant knowledge gap to determine the best optimized parameters for plasma processing. To increase the selectivity of products, a tandem PPT and convention catalysis bed may be used to push the reaction towards a desired direction.<sup>68–70</sup> Future study may concentrate on scaling, modeling, additional optimization for various product streams, varied clean and field-obtained feedstocks, catalytic effects of electrodes and added catalysts, and the lifetime of the reactor, among other research avenues.

Even under scenarios in which fossil fuels are phased out of the transportation sector, the existing petrochemical sector will require fossil-based feedstock for the foreseeable future. The flexibility of producing greener fossil-based feedstocks at a lower SEI with negligible GHG emissions will be a key technology for the energy transition.

## 8. Conclusion

The impact of plasma processing technology (PPT) in refineries was studied in this paper comparing the energy consumption, GHG emissions, and energy economics. Detailed comparative analysis and LCA were evaluated comparing the PPT with the traditional refinery configuration conversion FCC unit. Two different refinery configurations were selected with two different crude oil inputs. The medium conversion refinery was selected to process WTI while the deep conversion refinery was selected to process the heavy crude oil LLB. First, the energy consumption, GHG emissions, and energy cost of the traditional refineries were calculated with the data obtained from the PRELIM model. The plasma refining configuration was calculated incorporating results of work published by Wang *et al.*<sup>7</sup> The results were linearly extrapolated, and equivalent conversion was obtained to match the output of an FCC.

In general, a refinery incorporating a plasma process rather than an FCC consumes 14–18% more energy than a traditional refinery. This additional energy is a relatively small fraction <2% of the energy content of a barrel of oil. This energy is from the plasma process from renewable electricity and results in the

plasma process having 21–35% less GHG emissions. On a cost basis the plasma process is more expensive than traditional processing, but again, this is a small fraction of the total cost. Furthermore, in scenarios with a carbon tax, lower renewable energy costs, and improved plasma conversion efficiencies the cost of plasma processing can be lower than traditional processing and this can be an economically feasible and competitive model. A well to tank analysis was conducted for the plasma deep refinery configuration. Electrifying an upgrader using plasma in a deep refinery reduces emissions from 166 kg CO<sub>2eq</sub> per barrel of bitumen for the entire life cycle from well to tank to 148 kg CO<sub>2eq</sub> per barrel, a reduction of 11.5%. Integrating an industrial scale PPT in 1 major refinery in the US (e.g., Baytown Refinery in Texas owned by ExxonMobil with a capacity of 560 500 barrels per day) can result in a reduction of 5.6 million metric ton of CO<sub>2eq</sub> per year. Refineries represent 24% of all GHG emissions out of which 3.6% is from the petroleum industry. The total CO<sub>2</sub> emissions from the US in 2020 was 5.2 billion metric tons while the world emitted 18 billion CO<sub>2</sub> metric tons. The implementation in 1 refinery would lead to a 12% decrease in US refinery contributions to GHG, and an overall 0.1% decrease in US emissions. While this number may appear small, it is a substantial step towards reducing GHG emissions and remaining profitable in the energy transition. This paper provides a roadmap for an alternative green technology evaluation compared to BAU in a crude oil refining environment. Additionally, the economic feasibility of using PPT for fossil or biomass crude oil refining has been shown. PPT is a novel pathway in helping achieve net-zero GHG emissions to reduce the effects of climate change and to preserve our planet while satisfying the global energy demand profitably.

## Conflicts of interest

Aspects of this technology are patent pending technologies of the authors. US20210155855A1, US20210160996A1, US20210155856A1, and EP19788292.1. This work was sponsored by LTEOIL LLC under Texas A&M Engineering Experiment Station Project M2002860.

## Nomenclature

US	United States
BBL	Barrel
GHG	Greenhouse gas emissions
PPT	Plasma processing technology
FCC	Fluid catalytic cracking
TMR	Traditional medium refinery
PMR	Plasma medium refinery
TDR	Traditional deep refinery
PDR	Plasma deep refinery
WTI	West Texas intermediate
LLB	Lloydminster blend
WTT	Well to tank
WTW	Well to wheel
LCA	Life cycle analysis



PRELIM	Petroleum refinery life cycle inventory model
BAU	Business as usual
RFG	Refinery fuel gas
DBD	Dielectric barrier discharge
SEI	Specific energy input
API	American Petroleum Institute
NG	Natural gas
ADU	Atmospheric distillation unit
VDU	Vacuum distillation unit
AGO	Atmospheric gas oil
ATB	Atmospheric tower bottom
LVGO	Light vacuum gas oil
HVGO	Heavy vacuum gas oil
VTB	Vacuum tower bottom
CGO	Coker gas oil
CNR	Catalytic naphtha reformer
GO-HC	Gas oil hydrocracker
NHT	Naphtha hydrotreater
KHT	Kerosene hydrotreater
SAGD	Steam assisted gravity drainage
SAGD	Steam assisted gravity drainage
SCO	Synthetic crude oil
PSA	Pressure swing adsorption
SMR	Steam methane reforming
Dilbit	Diluted bitumen
GWP	Global warming potential
PPA	Power purchase agreement

## Acknowledgements

PRELIM software is owned by Dr Joule Bergerson of the University of Calgary, and she has granted permission to use the software for free. This work was sponsored by LTEOIL LLC under Texas A&M Engineering Experiment Station project M2002860.

## References

- U.S. Environmental Protection Agency, *Greenhouse Gas Reporting Program (GHGRP)*, U.S. EPA, 2017, <https://www.epa.gov/ghgreporting>.
- X. Tong, G. Zhang, Z. Wang, Z. Wen, Z. Tian, H. Wang, F. Ma and Y. Wu, Distribution and potential of global oil and gas resources, *Pet. Explor. Dev.*, 2018, **45**(4), 727–736.
- H. Wang, F. Ma, X. Tong, Z. Liu, X. Zhang, Z. Wu, D. Li, B. Wang, Y. Xie and L. Yang, Assessment of global unconventional oil and gas resources, *Pet. Explor. Dev.*, 2016, **43**(6), 925–940.
- Low Carbon Fuel Standard, California Air Resources Board, <https://ww2.arb.ca.gov/our-work/programs/low-carbon-fuel-standard>.
- Fuel Quality, [https://ec.europa.eu/clima/eu-action/transport-emissions/fuel-quality\\_en](https://ec.europa.eu/clima/eu-action/transport-emissions/fuel-quality_en).
- Specified Gas Reporting Regulation, Alberta.ca, <https://www.alberta.ca/specified-gas-reporting-regulation.aspx>.
- K. Wang, *et al.*, Electric fuel conversion with hydrogen production by multiphase plasma at ambient pressure, *Chem. Eng. J.*, 2021, 133660, DOI: [10.1016/j.cej.2021.133660](https://doi.org/10.1016/j.cej.2021.133660).
- T. Terlouw, K. Treyer, C. Bauer and M. Mazzotti, Life Cycle Assessment of Direct Air Carbon Capture and Storage with Low-Carbon Energy Sources, *Environ. Sci. Technol.*, 2021, **55**(16), 11397–1141.
- T. Shirvani, X. Yan, O. R. Inderwildi, P. P. Edwards and D. A. King, Life cycle energy and greenhouse gas analysis for algae-derived biodiesel, *Energy Environ. Sci.*, 2011, **4**, 3773–3778.
- S. Ramachandran and U. Stimming, Well to wheel analysis of low carbon alternatives for road traffic, *Energy Environ. Sci.*, 2015, **8**, 3313–3324.
- A. J. J. E. Eerhart, A. P. C. Faaij and M. K. Patel, Replacing fossil based PET with biobased PEF; process analysis, energy and GHG balance, *Energy Environ. Sci.*, 2012, **5**, 6407–6422.
- A. Shah, *et al.*, A review of novel techniques for heavy oil and bitumen extraction and upgrading, *Energy Environ. Sci.*, 2010, **3**, 700–714.
- B. Nimana, C. Canter and A. Kumar, Energy consumption and greenhouse gas emissions in upgrading and refining of Canada's oil sands products, *Energy*, 2015, **83**, 65–79.
- E. I. Nduagu and I. D. Gates, Unconventional Heavy Oil Growth and Global Greenhouse Gas Emissions, *Environ. Sci. Technol.*, 2015, **49**, 8824–8832.
- J. Charry-Sanchez, A. Betancourt-Torcat and L. Ricardez-Sandoval, An optimization energy model for the upgrading processes of Canadian unconventional oil, *Energy*, 2014, **68**, 629–643.
- B. Nimana, C. Canter and A. Kumar, Life cycle assessment of greenhouse gas emissions from Canada's oil sands-derived transportation fuels, *Energy*, 2015, **88**, 544–554.
- E. Delikontstantis, E. Igos, M. Augustinus, E. Benetto and G. D. Stefanidis, Production from rich-in-methane gas streams, *Sustain. Energy Fuels*, 2020, 1351–1362, DOI: [10.1039/c9se00736a](https://doi.org/10.1039/c9se00736a).
- E. Delikontstantis, M. Scapinello and G. D. Stefanidis, Process Modeling and Evaluation of Plasma-Assisted Ethylene Production from Methane, *Processes*, 2019, **7**, 68.
- A. Anastasopoulou, S. Butala, J. Lang, V. Hessel and Q. Wang, Life Cycle Assessment of the Nitrogen Fixation Process Assisted by Plasma Technology and Incorporating Renewable Energy, *Ind. Eng. Chem. Res.*, 2016, **55**(29), 8141–8153.
- R. G. Santos, W. Loh, A. C. Bannwart and O. V. Trevisan, An overview of heavy oil properties and its recovery and transportation methods, *Braz. J. Chem. Eng.*, 2014, **31**, 571–590.
- K. Guo, H. Li and Z. Yu, In-situ heavy and extra-heavy oil recovery: a review, *Fuel*, 2016, **185**, 886–902.
- J. Weitkamp, Catalytic Hydrocracking-Mechanisms and Versatility of the Process, *ChemCatChem*, 2012, **4**, 292–306.
- M. Fakhroleslam and S. M. Sadrameli, Thermal/catalytic cracking of hydrocarbons for the production of olefins; a state-of-the-art review III: process modeling and simulation, *Fuel*, 2019, **252**, 553–566.



24 S. M. Sadrameli, Thermal/catalytic cracking of hydrocarbons for the production of olefins: a state-of-the-art review I: thermal cracking review, *Fuel*, 2015, **140**, 102–115.

25 R. Sadeghbeigi, *Fluid Catalytic Cracking Handbook*, Fluid Catalytic Cracking Handbook, 2012, DOI: [10.1016/C2010-0-67291-9](https://doi.org/10.1016/C2010-0-67291-9).

26 A. Gutsol, A. Rabinovich and A. Fridman, Combustion-assisted plasma in fuel conversion, *J. Phys. D: Appl. Phys.*, 2011, **44**, 274001.

27 M. G. Warawdekar, Challenges in Scale-Up of Specialty Chemicals-A Development Chemist's Perspective, in *Industrial Catalytic Processes for Fine and Specialty Chemicals*, 2016, DOI: [10.1016/B978-0-12-801457-8.00016-1](https://doi.org/10.1016/B978-0-12-801457-8.00016-1).

28 K. Hadidi, *et al.*, *Plasma Catalytic Reforming of Biofuels*, Plasma Sci. Fusion Center, 2003, vol. 3.

29 G. Petipas, *et al.*, A comparative study of non-thermal plasma assisted reforming technologies, *Int. J. Hydrogen Energy*, 2007, **32**(14), 2848–2867.

30 A. Khosravanipour Mostafazadeh, O. Solomatnikova, P. Drogui and R. D. Tyagi, A review of recent research and developments in fast pyrolysis and bio-oil upgrading, *Biomass Convers. Biorefin.*, 2018, **8**(3), 739–773.

31 H. Hao, *et al.*, Non-thermal plasma enhanced heavy oil upgrading, *Fuel*, 2015, **149**, 162–173.

32 S. Timmerberg, M. Kaltschmitt and M. Finkbeiner, Hydrogen and hydrogen-derived fuels through methane decomposition of natural gas – GHG emissions and costs, *Energy Convers. Manage.: X*, 2020, **7**, 100043.

33 J. H. Harrhy, *et al.*, Understanding zeolite deactivation by sulfur poisoning during direct olefin upgrading, *Commun. Chem.*, 2019, **2**, 44.

34 M. D. Argyle and C. H. Bartholomew, Heterogeneous catalyst deactivation and regeneration: a review, *Catalysts*, 2015, **5**, 145–269.

35 K. Rajashekara, Electrification of Subsea Systems Requirements and Challenges in Power Distribution and Conversion, *CPSS Trans. Power Electron. Appl.*, 2017, **2**, 04.

36 J. I. Marvik, E. V. Øyslebø and M. Korpås, Electrification of offshore petroleum installations with offshore wind integration, *Renew. Energy*, 2013, **50**, 558–564.

37 L. Riboldi, S. Völler, M. Korpås and L. O. Nord, An integrated assessment of the environmental and economic impact of offshore oil platform electrification, *Energies*, 2019, **12**, 2114.

38 M. Wei, *et al.*, Deep carbon reductions in California require electrification and integration across economic sectors, *Environ. Res. Lett.*, 2013, **8**, 014038.

39 S. Madeddu, *et al.*, The CO<sub>2</sub> reduction potential for the European industry via direct electrification of heat supply (power-to-heat), *Environ. Res. Lett.*, 2020, **15**, 124004.

40 A. Indarto, J. W. Choi, H. Lee and H. K. Song, Decomposition of greenhouse gases by plasma, *Environ. Chem. Lett.*, 2008, **6**(4), 215–222.

41 A. Fridman, *Plasma Chemistry*, 2008, ISBN no. 9780521847353.

42 Y. P. Raizer, *Gas Discharge Physics*, IEE Colloquium (Digest), 1991.

43 J. Meichsner, M. Schmidt, R. Schneider and H. E. Wagner, *Nonthermal Plasma Chemistry and Physics*, 2012, DOI: [10.1201/b12956](https://doi.org/10.1201/b12956).

44 M. R. Khani, *et al.*, Investigation of cracking by cylindrical dielectric barrier discharge reactor on the n-hexadecane as a model compound, *IEEE Trans. Plasma Sci.*, 2011, **39**(9), 1807–1813.

45 G. Prieto, *et al.*, A plate-to-plate plasma reactor as a fuel processor for hydrogen-rich gas production, in *Conference Record – IAS Annual Meeting*, IEEE Industry Applications Society, 2001, vol. 2.

46 A. Jahanmiri, M. R. Rahimpour, M. Mohamadzadeh Shirazi, N. Hooshmand and H. Taghvaei, Naphtha cracking through a pulsed DBD plasma reactor: Effect of applied voltage, pulse repetition frequency and electrode material, *Chem. Eng. J.*, 2012, **191**, 416–425.

47 M. R. Khani, A. Khosravi, E. Dezhbangooy, B. M. Hosseini and B. Shokri, Study on the feasibility of plasma (DBD Reactor) cracking of different hydrocarbons (n-Hexadecane, Lubricating Oil, and Heavy Oil), *IEEE Trans. Plasma Sci.*, 2014, **42**(9), 2213–2220.

48 Y. Matsui, S. Kawakami, K. Takashima, S. Katsura and A. Mizuno, Liquid-Phase Fuel Re-forming at Room Temperature Using Nonthermal Plasma, *Energy Fuels*, 2005, **19**(4), 1561–1565.

49 K. Rathore, S. I. Bhuiyan, S. M. Slavens and D. Staack, Microplasma ball reactor for JP-8 liquid hydrocarbon conversion to lighter fuels, *Fuel*, 2021, **285**, 118943.

50 K. Wang, *et al.*, CO<sub>2</sub> -free conversion of fossil fuels by multiphase plasma at ambient conditions, *Fuel*, 2021, **304**, 121469.

51 K. Wang, S. I. Bhuiyan, M. A. H. Baky, J. Kraus, C. Campbell, X. Tang, H. Jemison and D. Staack, Role of bubble and impurity dynamics in electrical breakdown of dielectric liquids, *Plasma Sources Sci. Technol.*, 2021, **30**(5), 055013.

52 K. Wang, S. I. Bhuiyan, M. A. Hil Baky, J. Kraus, C. Campbell, H. Jemison and D. Staack, Relative breakdown voltage and energy deposition in the liquid and gas phase of multiphase hydrocarbon plasmas, *J. Appl. Phys.*, 2021, **129**(12), 123301.

53 K. Wang, D. Staack, H. Jemison, S. I. Bhuiyan and C. Martens, *Heavy Oil Cracking Device Scaleup with Multiple Electrical Discharge Modules*, 2021.

54 F. J. Keil, Process intensification, *Rev. Chem. Eng.*, 2018, **34**, 135–200.

55 J. P. Abella, K. Motazed, J. Guo, K. Cousart and J. A. Bergerson, Petroleum Refinery Life Cycle Inventory Model (PRELIM), *PRELIM v1.3 User Guide and Technical Documentation*, University of Calgary, 2019.

56 J. P. Abella and J. A. Bergerson, Model to investigate energy and greenhouse gas emissions implications of refining petroleum: Impacts of crude quality and refinery configuration, *Environ. Sci. Technol.*, 2012, **46**, 13037–13047.

57 S. Ong, C. Campbell, P. Denholm, R. Margolis and G. Heath, *Land-Use Requirements for Solar Power Plants in the United States*, 2013, NREL/TP-6A20-56290.



58 U.S. Energy Information Administration – EIA, *Independent Statistics and Analysis*, [https://www.eia.gov/todayinenergy/detail.php?id=45476&fbclid=IwAR2UMKlvWex9dSUATRhFeCjh3lxBRjXN3lo3-aXKE92vPQQhy\\_ZkEN1Kc](https://www.eia.gov/todayinenergy/detail.php?id=45476&fbclid=IwAR2UMKlvWex9dSUATRhFeCjh3lxBRjXN3lo3-aXKE92vPQQhy_ZkEN1Kc).

59 *Barrel of Oil Equivalent (BOE) Definition*, <https://www.investopedia.com/terms/b/barrelofoilequivalent.asp>.

60 *Prices and factors affecting prices*, U.S. Energy Information Administration (EIA), <https://www.eia.gov/energyexplained/electricity/prices-and-factors-affecting-prices.php>.

61 *Wind Power*, <https://www.irena.org/costs/Power-Generation-Costs/Wind-Power>.

62 *U.S. Natural Gas Prices*, [https://www.eia.gov/dnav/ng/ng\\_pri\\_sum\\_deu\\_nus\\_m.htm](https://www.eia.gov/dnav/ng/ng_pri_sum_deu_nus_m.htm).

63 *Gasoline and Diesel Fuel Update*, U.S. Energy Information Administration (EIA), <https://www.eia.gov/petroleum/gasdiesel/>.

64 *The Economic Value of Renewable Energy in Texas, Fall 2018*.

65 *Short-Term Energy Outlook*, U.S. Energy Information Administration (EIA), <https://www.eia.gov/outlooks/steo/report/prices.php>.

66 M. Bruck, P. Sandborn and N. Goudarzi, A Levelized Cost of Energy (LCOE) model for wind farms that include Power Purchase Agreements (PPAs), *Renewable Energy*, 2018, **122**, 131–139.

67 *Use of oil*, U.S. Energy Information Administration (EIA), <https://www.eia.gov/energyexplained/oil-and-petroleum-products/use-of-oil.php>.

68 E. C. Neys and A. Bogaerts, Understanding plasma catalysis through modelling and simulation – a review, *J. Phys. D: Appl. Phys.*, 2014, **47**, 224010.

69 I. Istadi, A. D. Yudhistira, D. D. Anggoro and L. Buchori, Electro-catalysis system for biodiesel synthesis from palm oil over Dielectric-Barrier Discharge plasma reactor, *Bull. Chem. React. Eng. Catal.*, 2014, **9**, 111–120.

70 H. H. Kim, Y. Teramoto, A. Ogata, H. Takagi and T. Nanba, Plasma Catalysis for Environmental Treatment and Energy Applications, *Plasma Chem. Plasma Process.*, 2016, **36**, 45–72.

